



**UNIVERSITÀ  
DEGLI STUDI DI BARI  
ALDO MORO**

**DIPARTIMENTO DI SCIENZE AGRO AMBIENTALI E TERRITORIALI**

**CORSO DI LAUREA MAGISTRALE IN SCIENZE AGRO-AMBIENTALI E TERRITORIALI**

---

**Tesi di Laurea Magistrale in**

**ARBORICOLTURA GENERALE E COLTIVAZIONI ARBOREE**

**Suitabox: An ArcGIS® toolbox to assess the distribution suitability of tree crops  
based on air temperature data**

**Relatori:**

**Chiar.mo Prof. Gaetano Alessandro VIVALDI**

**Dr. Juan Miguel RAMIREZ-CUESTA**

**Correlatori:**

**Dr. Diego S. INTRIGLIOLO**

**Dr. Juan Gabriel PÉREZ PÉREZ**

**Controrelatore:**

**Chiar.mo Prof. Giuliano VOX**

**Laureando:**

**Francesco PASANISI**

---

**Anno Accademico 2020-2021**



# Table of Contents

<b>Introduction .....</b>	<b>4</b>
<b>Methods .....</b>	<b>7</b>
Suitabox implementation .....	7
Crop Suitability tool .....	8
General inputs and core operations.....	9
Custom periods .....	12
Climate change scenarios.....	13
Interpolation settings .....	14
Output settings.....	14
Suitabox practical application .....	17
<b>Results .....</b>	<b>22</b>
The primary output types.....	22
The additional outputs .....	23
The topographic correction .....	25
Climate change projections .....	27
<b>Discussion.....</b>	<b>30</b>
<b>Conclusions .....</b>	<b>35</b>
<b>References.....</b>	<b>36</b>
<b>Supplementary material .....</b>	<b>42</b>

## **1. Introduction**

One of the most concerning issues of society is the restricted ability of the world's natural resources to satisfy the needs of the population. Essential natural resources, such as land and water, are declining both in quantity and quality due to several factors such as overexploitation, competition among different sectors, degradation, and pollution (FAO, 1996). Being the agricultural sector the principal world's food supply source and a crucial factor for countries' development, the application of efficient management techniques for natural resources is considered a priority for the sustainability of agricultural production processes (Dengiz, 2013). In a context of global and constant demographic growth, climate change and over-exploitation of the available natural resources, the management and selection of the most convenient zones of strategically valuable crops are extremely critical to develop sustainable agriculture policies (Tercan and Dereli, 2020).

Many research works concerning the selection of suitable sites for different activities have been published in the last decade. Selim et al. (2018) performed the site selection for avocado cultivation using GIS and multi-criteria decision analysis (MCDA) in Antalya (Turkey) territory, Allaw and Al-Shami (2018) produced some GIS-based maps for the agricultural management of South-Lebanon, Hazain et al. (2012) realized a land suitability WebGIS for agricultural purpose in Indonesia. However, most of the site-selection and land suitability studies in the literature use one or more MCDA techniques, such as weighted overlay, analytical hierarchy process (AHP), and analytical network process (ANP). In these papers, authors usually consider some climate, topographic, and soil parameters and focus their attention on only one crop species, but Elseikh et al. (2013) presented ALSE (Agriculture Land Suitability Evaluator), an expert system capable of automating the assessment of land suitability for different crops in tropical and subtropical regions based on geo-environmental factors and using computer modeling, GIS and multi-criteria analysis.

One of primary factor determining crops' development and success is climate. Indeed, plants need an adequate growing season for the accomplishment of all phenological stages (Ramankutty et al., 2002).

Climate influence the distribution of plants, as recognized by several studies (Holdrige, 1967; Box, 1981; Woodward and Williams, 1987). Moreover, Iizumi and Ramankutty (2015) stated that climate and weather influence crops in different ways, considering that a fatal event to crops that takes place during the growth period is more relevant than the general conditions during the growing season; however, if there are no fatal events the mean conditions of growing season represent a reliable factor to explain the differences in crops' production. Furthermore, the authors underline how the influence of weather and climate on crops' production can vary, and the actual climatic influences are quite complex.

Concerning the different climatic variables, Hatfield and Prueger (2015) indicate that air temperature is a primary factor affecting the rate of plant development, and each species has a specific temperature range represented by a minimum, maximum and optimum. The authors underline the crops' responses to temperature are related to their life cycle and are primarily phenological responses, affecting the plant development, and that one of the most temperature-susceptible phenological stages is represented by pollination. Furthermore, many perennial crops that originated in temperate climates have a chilling requirement in which plants have to be exposed to a certain number of hours below a defined threshold (depending on the model adopted) during the dormancy period; if the minimum number of hours required by the crops is not achieved, it compromises the normal vegetative and flower budbreak, provoking production losses. This shows the primary importance of air temperature for crops, affecting the plant development during the growing season but also during the dormancy of some perennial crops.

Geographic Information Systems (GIS) is a technology capable of integrating different information sources at a spatial level. In the last few decades, GIS have gone through a strong technological evolution, significantly improving land analysis and management methods. Indeed, their main feature is their multidisciplinary nature, allowing people to use them in several research and work environments: geology, environmental monitoring, heritage and archeology, agronomy and forestry,

technological infrastructures, etc. Their recent success is the consequence of the gradual transition from the strict cartographic approach (map-oriented) to a digital and quantitative way of use (GIS-oriented) characterized by data organization in logical layers, connected to a descriptive component (database). This shift happened thanks to the increasing data availability and the evolution of hardware and software instruments (Noti, 2014). For all these reasons, GIS have proved to be a useful software environment in land-use planning and agricultural land suitability, providing technology and a suite of tools for achieving the above-mentioned tasks and, especially, converting variables that are non-spatial to obtain spatial-related data.

To the best of our knowledge, GIS environment and ArcGIS toolboxes have never been used in the literature to create tools able to perform a distribution suitability studies of new tree crop species within areas in which they are marginally or not cultivated. Furthermore, most of the above-cited models and methodologies are too complex for non-specialized users, as in the case of many farmers and decision-makers, and even by more qualified users such as GIS technicians. To solve the above-mentioned limitations, in this work we present Suitabox, an open-source and user-friendly ArcGIS toolbox helpful to carry out suitability mapping for tree crops in Mediterranean areas. Suitabox main script tool is a simple instrument that uses hourly temperature data, collected from weather stations, and elevation to find suitable areas for the cultivation of a specific crop, according to some agroecological thresholds. At this time, Suitabox implements only temperature and elevation without using soil data or other climate variables to ensure simplicity for every kind of user. The usefulness of the proposed toolbox is to perform preliminary studies at a regional scale about the suitability of a considered crop in a fast and automated way.

## **2. Methods**

### ***2.1. Suitabox implementation***

In this study, Suitabox has been developed by using Python and ArcPy library, embedded in ArcGIS (Arcmap v10.5, ArcGIS Pro 2.9; Esri, Redlands, CA, USA). ArcPy provides access to ArcGIS geoprocessing tools as well as to existing functions, modules, and classes in order to develop powerful scripts thanks to its code-completion function and the function-specific reference documentation. Moreover, the use of Python programming language permits benefiting from the development of additional modules by GIS professionals and programmers (Ramirez-Cuesta et al., 2020).

The toolbox consists of 2 different script tools: Crop Suitability Tool and Custom Pre-Processing. Figure 1 shows the flowchart and the interrelationship between the different modules. In the next subsection, a detailed explanation of each script tool is provided.

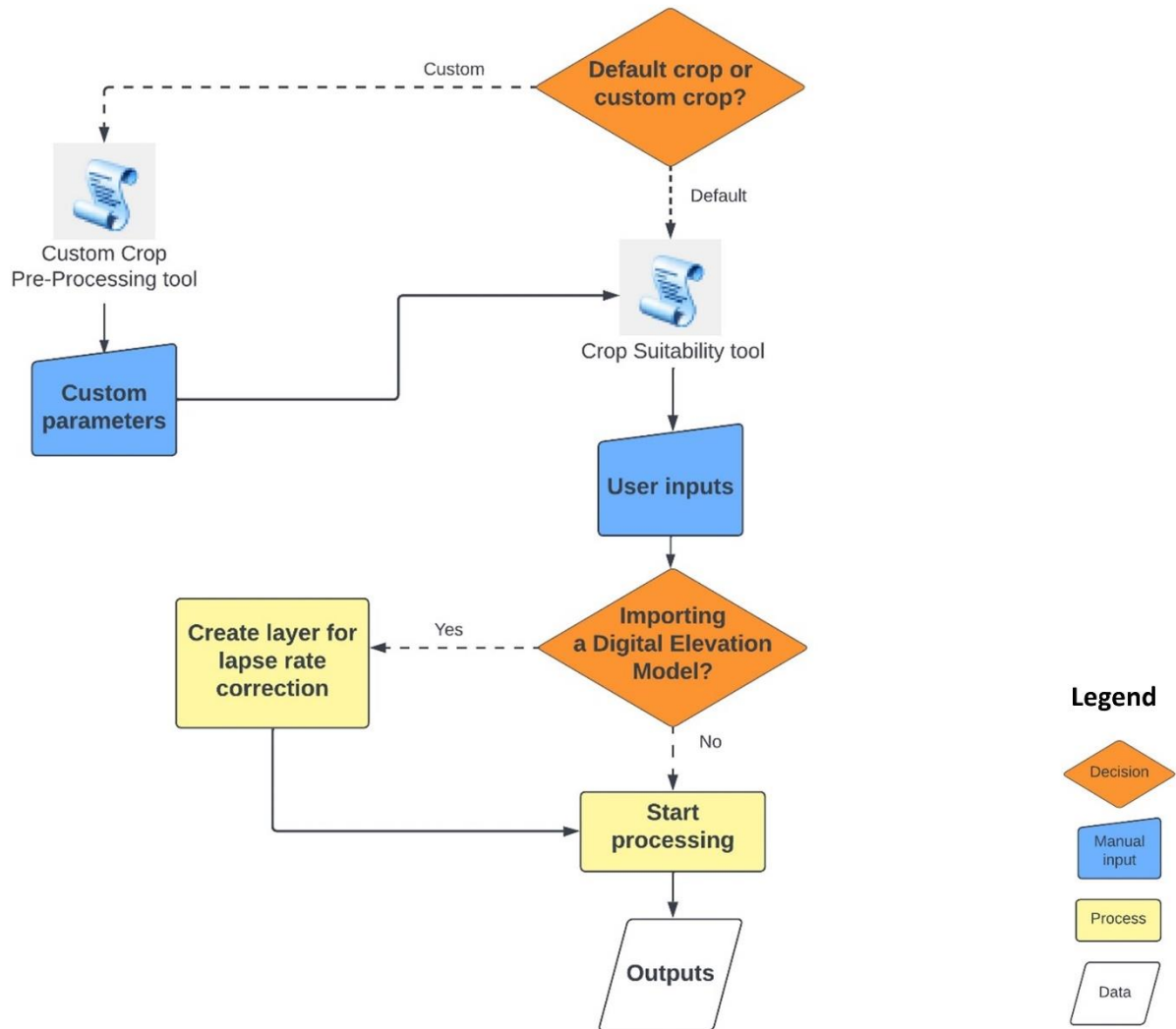


**Figure 1.** Flowchart showing the core procedure of Suitabox.

### 2.1.1. Crop Suitability tool

This script tool is the core of Suitabox. Its main purpose is to produce, for a given area of study and meteorological conditions, a suitability map of the considered crop species.

The inputs required to the user in the Crop Suitability tool have been divided into 5 categories: i) General inputs, ii) Custom periods, iii) Climate change scenarios, iv) Interpolation settings and v) Output settings (Fig 2a and b).



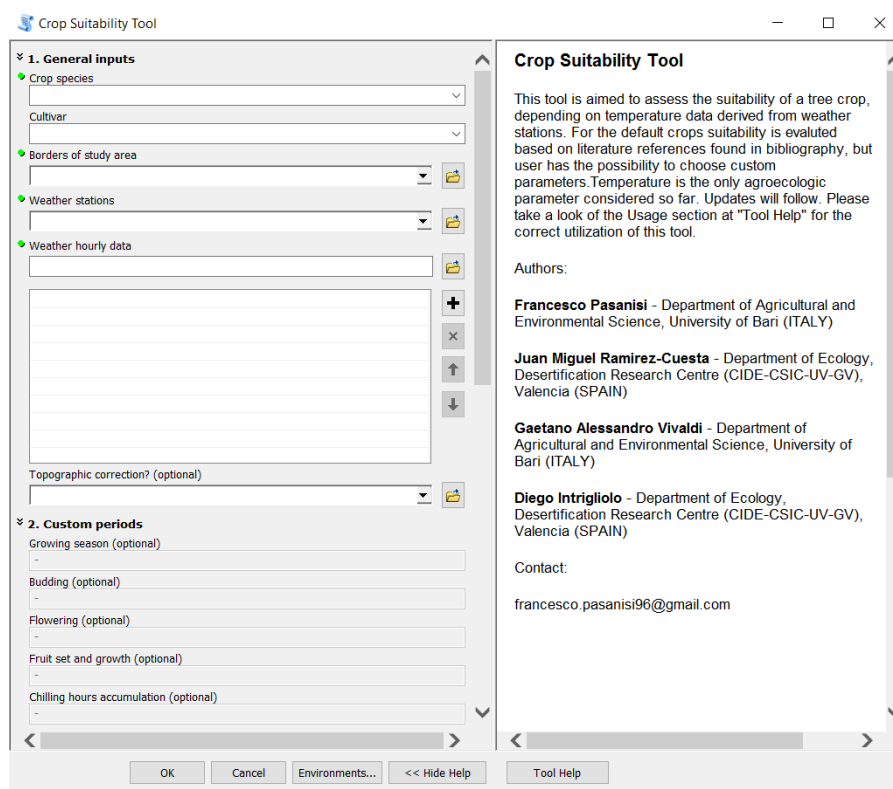


**Figure 2.** Section two of the Crop Suitability Tool user interface, implemented in ArcGIS shows the different input parameters and standard default parameter values. Readers are referred to the main text for the explanation of each input parameter.

#### 2.1.1.1. General inputs and core operations

Within the *General inputs* category (Figure 2), the user is asked to specify:

- 1) Crop species: the user can choose one of the default crop species included in the toolbox, or to include a customized one using the *Custom crop* option (see Section “2.1.2. Custom Crop Pre-Processing”). The considered default crop species are avocado (*Persea americana* Milil.), kiwifruit (*Actinidia* sp.), walnut (*Juglans regia* L.) and European hazelnut (*Corylus avellana* L.). For each one of these crops, different temperature thresholds or requirements have been identified based on literature references (Tables S1-S4) and implemented within the code.
- 2) Cultivar (required depending on the selected crop species). This input is essential since some of the air temperature thresholds or requirements are cultivar specific (Tables S1-S4).

- 3) Borders of the study area: an ESRI polygon shapefile (.shp) with the extension of the study area. This input serves to shorten processing time and computational resource consumption.
- 4) Weather stations: A point feature layer (.shp) containing the weather stations location. The feature attribute table must have an *ID* column with an integer and unique number for each station. If the user wants to use the *topographic correction* option (explained in point 6), this shapefile must also have an additional column (named *alt*) with the altitude in meters of each meteorological station.
- 5) Weather hourly data. This input refers to a dataset, obtained from the weather stations, with hourly resolution. The user can upload one dataset per year. This dataset must have the following columns: i) an *ID* column to be joined with the weather stations layer, in integer type; ii) a Day of Year (*DoY*) column in integer type; iii) an air temperature (*Tair*) column with the temperature data. If the user selects a crop with a winter chilling hours requirement (i.e. kiwifruit, walnut, hazelnut, or custom crop; Tables S1-S4) the dataset must cover a hydrological year (i.e., from 01 October of year *n* to 30 September of year *n*+1) to refer the chilling hours' calculation to that specific season.
- 6) Topographic correction. Optionally, the user can upload a Digital Elevation Model (DEM) raster layer where the tool wizard asks for topographic correction. If provided, the script tool will compute a correction of the interpolated air temperature using the terrain altitude. The temperature will be corrected (*Tair.corr*) using the following formula, which applies the average environmental lapse rate factor (6.5 °C km<sup>-1</sup>; Barry and Chorley, 1987) through a DEM obtained via interpolation of the *altitude* (*alt*) field of the weather stations layer (DEMint):

$$Tair.corr = Tair.int + (DEM.diff) * 0.0065 \quad (1)$$

where  $T_{air,int}$  (°C) is the air temperature obtained interpolating the values measured in the weather stations, and  $DEM.diff$  is calculated by the difference between the interpolated DEM ( $DEM.int$ ) and the original DEM ( $DEM.original$ ):

$$DEM.diff = DEM.int - DEM.original \quad (2)$$

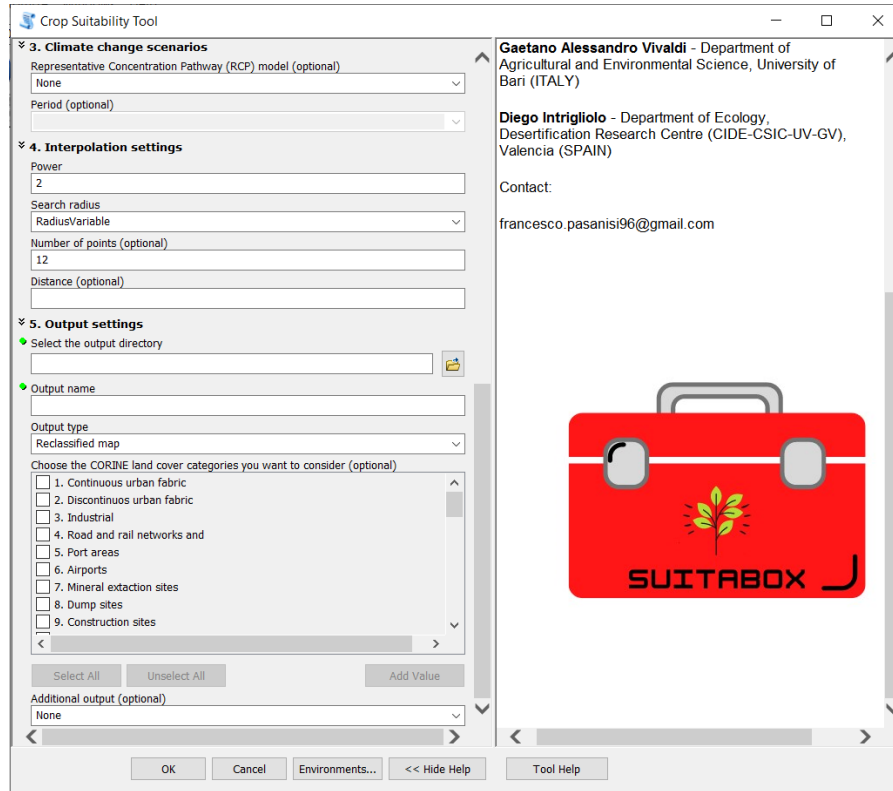


**Figure 3.** Section two of the Crop Suitability Tool user interface, implemented in ArcGIS shows the different input parameters and standard default parameter values. Readers are referred to the main text for the explanation of each input parameter.

To carry out the different functions, the program follows these subsequent steps (Figure S3):

1. After the principal routine has acquired the user's inputs, depending on the selected crop species a specific subroutine is called.
2. The subroutine creates a dataframe for each parameter required by the considered crop species (Table S1-S4), which is made by two columns: *ID*, related to the weather station, and a second column that shows the temperature data of interest.

3. Each of these dataframes is merged into one single dataframe. Through a full join operation, this final dataframe is joined to the weather stations' points and the interpolation is executed for each parameter, obtaining a set of interpolated raster layers.
4. The interpolated layers go through a reclassification process, based on the crops' requirement table. Each value range corresponds to a score: 0, 0.25, 0.75 or 1.
5. The multiplication of the reclassified layers is executed in order to obtain a provisional suitability layer, in which pixels have a value between 0 and 1. This process is performed by the subroutine for each weather dataset imported by the user, resulting in a list of annual suitability layers.
6. The calculation of the average among the annual suitability layers is executed and the final suitability map is obtained.

#### **2.1.1.2. Custom periods**

Within the *Custom periods* category (Figure 2), the user can change for each specific phenological phase (i.e. growing season, budding, flowering, fruit set and growth, chilling hours accumulation) the DoY range considered to extract the Tair data needed for evaluating the thresholds/requirements of the default tree crops. By default, the considered periods are the ones included in Table 1. The user should include the initial and final DoY separated by a hyphen. If the user does not modify the text inside these boxes (i.e., leaving the hyphen inserted by default), the standard periods will be used. As shown in Table 1, not all the considered periods are related to each default crop, depending on the literature references found in bibliography so far, i.e., when the user selects a crop species only some specific periods will be customizable.

Table 1. Time periods (expressed in DoY) for the considered phenological stage of default crops.

Crop species	Growing season	Budding	Flowering	Fruit set and growth	Chilling accumulation	hours
Avocado			60-151	152-365		
Kiwifruit		60-151	121-151		274-46	
European hazelnut					274-46	
Walnut	91-305				274-46	

### 2.1.1.3. Climate change scenarios

Climate science organizations worldwide generate future climate models based on Representative Concentration Pathway (RCP) scenarios. An RCP represents a greenhouse gas concentration trajectory compatible with the full range of emissions scenarios available in the current scientific literature, with and without climate policy (van Vuuren et al., 2011a).

In the fifth Assessment Report (IPCC, 2014), IPCC adopted four standard RCPs with GHG concentrations that add the following levels of radiative forcing: 2.6, 4.5, 6.0, and 8.5 W/m<sup>2</sup>. These scenarios give a range from best (2.6) to worst (8.5) case for adding GHGs into the atmosphere:

- RCP 2.6: Radiative forcing levels not only peak prior to but also decline to 2.6 W m<sup>-2</sup> by 2100.
- RCP 4.5: Radiative forcing levels stabilize without exceeding 4.5 W m<sup>-2</sup> by 2100. Scenario 4.5 is still considered a realistic possibility.
- RCP 6.0: Radiative forcing levels stabilize without exceeding 6.0 W m<sup>-2</sup> by 2100. Scenario 6.0 is also considered a realistic possibility.
- RCP 8.5: Radiative forcing levels are modeled with different assumptions than 2.6, 4.5, and 6.0, reaching 8.5 W m<sup>-2</sup>.

Within the *Climate change scenarios* category of Suitabox (Figure 3), the user can optionally consider one of the available RCP models to simulate the crop suitability distribution under such scenarios (Amman et al., 2018). If this option is used, the Tair of each weather station will be corrected with the annual average temperature rise predicted by the chosen scenario within the pixel where the weather station is located (Amman et al., 2018). Furthermore, the user can select different temporal windows: the near-future (period 2020-2039) and increasingly distant-future projection (periods 2040-2059, 2060-2079, 2080-2099).

#### **2.1.1.4. Interpolation settings**

The interpolation method used in Suitabox is the Inverse Distance Weighting (IDW) approach, due to its simplicity and good performance as shown by various studies (Chen and Liu, 2012; Moeletsi et al., 2016; Ramirez-Cuesta et al., 2017). The IDW method is a deterministic spatial interpolation model, whose general premise is that the attribute values of any given pair of points are related to each other, but their similarity is inversely related to the distance between the two locations (Lu et al., 2008).

Despite the simplicity of IDW method, this method requires fixing the value of some parameters (power, search radius, and the number of points). As readers can see in Figure 3, the default values of the core parameters of the IDW tool in ArcGIS are automatically set. However, within the *Interpolation settings* category, a most experienced user can customize these values depending on the necessities. The IDW interpolation approach is described in detail in Li and Heap (2008, 2011).

#### **2.1.1.5. Output settings**

Finally, within the *Output settings* category (Figure 3) the user can:

- 1) Select the output directory. Suitabox will use the information from this input to create a new folder inside the selected path, named “{output name}\_output”.

- 2) Write the output name, for specifying the nomenclature of the file to be created inside the output folder.
- 3) Select the output type. The user can choose between the “Reclassified map” and the “Stretched values map”. The first one is obtained by doing a final reclassification of the suitability map according to the 4 classes shown in Table 2 (0 for excluded areas and 1-4 from Unsuitable to Highly Suitable). The second option, “Stretched values map”, is obtained without executing the final reclassification therefore showing stretched values from 0 to 1, an area being more suitable when closer to 1. Furthermore, the user can decide to exclude some land uses from the map (such as non-agricultural areas) using CORINE Land Cover (Copernicus Land Monitoring, 2022). This option is only available for regions covered by CORINE. The user is provided with a multiple-choice box list, where is possible to select the desired areas. By default, agricultural areas are selected. The tool will apply a specific symbology to the final map depending on the selected output type.
- 4) Additional output. Optionally, the user can select an additional output between a Standard Deviation map and an Uncertainty map. The first one is computed by calculating the standard deviation among the provisional suitability layers, to visualize the variations of a certain pixel. The Uncertainty map shows the spatial uncertainty of the obtained map, and it is computed depending on the weather stations’ location and distance, using the Euclidean Distance function of the ArcGIS Spatial Analyst toolbox. This function calculates, for each cell, the Euclidean distance to the closest weather station. The purpose of this additional map is to underline the uncertainties in the toolbox output as a consequence of the closest weather station distance.

Table 2. Considered classes for obtaining the “Reclassified map” output type. The  $x$  symbol represents the pixel value of the suitability map.

Class		Excluded areas	Unsuitable	Marginally suitable	Suitable	Highly suitable
<b>Stretched value</b>	<b>pixel</b>	Unsuitable land uses (CLC)	$0 \leq x < 0.25$	$0.25 \leq x < 0.50$	$0.50 \leq x < 0.75$	$x \geq 0.75$
<b>Reclassified value</b>	<b>pixel</b>	0	1	2	3	4

Once the processing is completed, the outputs selected by the user are automatically uploaded to the ArcGIS canvas. The user can find the related files inside the working directory, as well as the provisional suitability layers and the dataframes used by the subroutine to execute the interpolation, created for each weather dataset imported. The raster layers obtained will have the same spatial resolution as the Digital Elevation Model provided by the user; whereas a default spatial resolution of 100 m will be used if it is not uploaded.

### 2.1.2. Custom Crop Pre-processing

This tool (Figure 4) is preparatory for the use of the *Custom crop* option in the Crop Suitability tool. The purpose of this tool is to prepare a table with the custom crop’s requirements defined by the user, which will be exported as a CSV file inside the toolbox directory and read by the Crop Suitability tool subroutine specific for the *Custom crop* option.

In the *param\_name* column, the user should write the desired parameter name, preferably without spaces. In the *param\_ID* column, the user must provide an integer ID, possibly incrementing this number by one for each parameter uploaded. In the *function* column, the user writes a specific function to apply for the calculation of the related custom parameter. These functions’ calculations are grouped for each weather station and are related to a specific period. At the moment, there are 6 available functions: *mean*, *min*, and *max* calculate the average, minimum, and maximum Tair; *avg\_daily\_max* and *avg\_daily\_min* calculate, respectively; the average of daily maximum and



minimum T; finally, the *chill\_hours* function executes a count of the chilling hours according to Weinberger (1950). To use this function, subsequently, the user should upload a weather dataset in hydrological year format inside the Crop Suitability tool.

In the *doy\_range* column, the user defines the period of time of interest to extract the weather data, expressed in DoY. The starting and the ending DoY must be separated by a hyphen.

In the last 4 columns (*unsuitable*, *marginal*, *suitable*, *highly\_suit*) the user can specify the value ranges for each class. The two extremes of the range must be separated by a semicolon. To express a range that tends to  $\pm$ infinity, the use of a great absolute number (positive or negative) is necessary in order to cope with the ArcPy function used to accomplish this task (e.g., in Figure 4,  $\pm 999$  has been used for this reason).

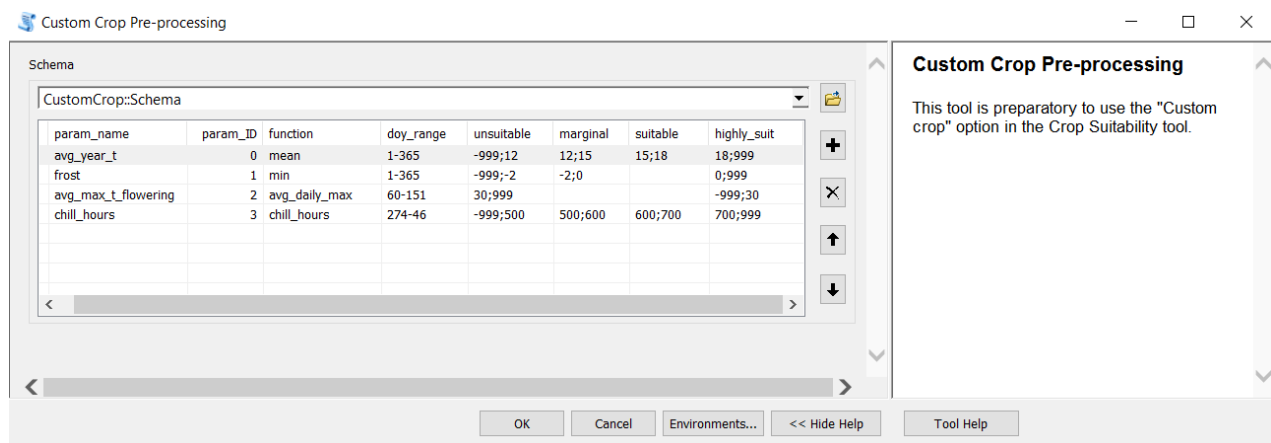


**Figure 4.** The Custom Crop Pre-processing wizard, with an example of how to fulfill the custom crop parameters table.

## 2.2. Suitabox practical application

The toolbox has been tested in order to show its different outputs and their changes according to different user inputs. A practical application has been performed at the Valencian Community located along the Mediterranean coast on the east side of the Iberian Peninsula (Figure 5). Tree crop production is one of the most important agricultural activities, especially citrus cultivation (Table 3). In addition, Valencian Community has roughly 493,407 ha of land covered by tree crop orchards, divided into citrus, non-citrus tree crops, olive grove, vineyard, and other minor crops (MAPA, 2020).

For this practical application, avocado (*Persea americana* Milil.) has been used as crop species. The choice of this tree crop comes from the increasing interest of Valencian farmers in this crop, its future market prospects, and potential profitability. This increase is driven by rising worldwide demand and significant investments in production. Furthermore, avocado is cultivated only in a few zones within the study area, especially in the south-eastern area near the coast; therefore, the selection of suitable sites for its cultivation may be helpful to stimulate the presence of a different crop, on both farm and territorial levels, thus taking advantage of the enormous benefits that agricultural diversification can provide (Ijaz et al., 2019).

The cartographic data concerning the study area (i.e., DEM and administrative borders shapefile) were obtained from the Autonomous body National Center for Geographic Information (CNIG, 2022 - <https://centrodedescargas.cnig.es>).

The weather stations shapefile and the related datasets were obtained from the Agroclimatic Information System for Irrigation (SiAR, <https://datos.gob.es/en/blog/agroclimatic-information-system-irrigation-siar>) network of the Valencian Community, managed by the Valencian Institute for Agricultural Research (IVIA, <http://riegos.ivia.es/red-siar>). In Valencian Community, this network currently includes stations distributed within all the areas where irrigated crops are located, providing valuable open datasets for the agricultural sector. For this practical application, a period of five years of hourly data, from 2016 to 2020, of 41 agro-climatic stations of this network have been used (Figure 5).

In the test case, the 4 different output types (Stretched values map, reclassified map, stretched values map with CLC, reclassified map with CLC) were examined to show the differences among them. Also, both additional outputs (Standard deviation map and Uncertainty map) have been evaluated. A comparison between the output derived from the use of the *topographic correction* option and the opposite case was carried out in order to visualize the usefulness of this option. For this application, a DEM of the study area with a spatial resolution of 100 m was used. Furthermore, the application of

two RCP models, the best-case and the worst-case scenarios (respectively, RCP2.6 and RCP8.5), has been carried out to show the discrepancies between the current status and the predictions for the future periods (2020-2039, 2040-2059, 2060-2079, 2080-2099). The default interpolation settings were used for all the applications.

Finally, the application of a proposed method for chilling hours correction (explained in the following paragraph, 2.3). This feature was tested on kiwifruit (cultivar: Jinyan) because a crop species with winter chilling requirement was necessary.

Table 3. Valencian Community acreage of the principal tree crops (PEGV, 2020 — <https://pegv.gva.es/va/inicio>).

<b>Crop group</b>	<b>Acreage (ha)</b>
Citrus	161,236
Non-citrus tree crops	132,098
Vineyard	64,079
Olive grove	93,953
Other minor tree crops	18,510

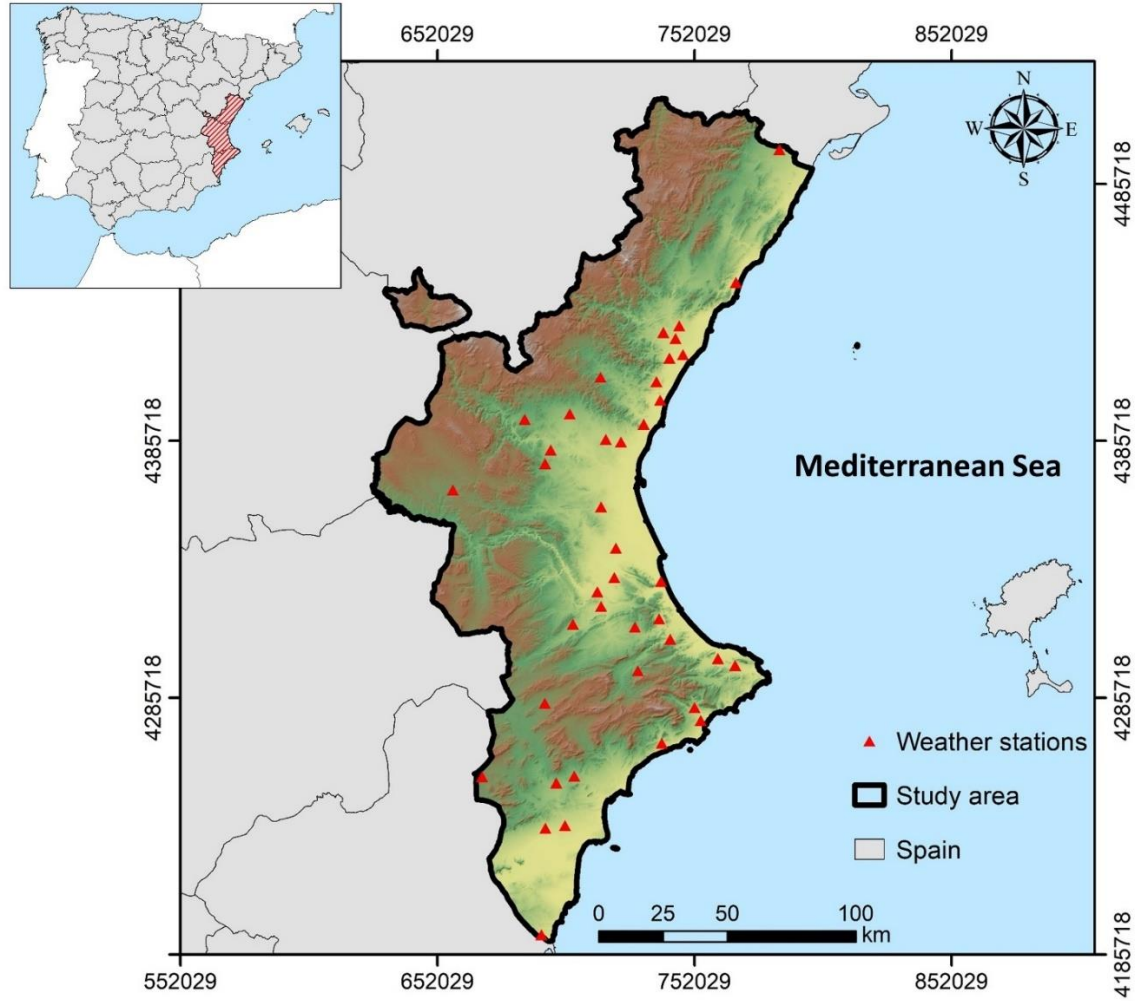


**Figure 5.** Study area considered in the test case (Coordinate Reference System: ETRS 1989 UTM zone 33N). Valencian Community located along the Mediterranean coast on the east side of the Iberian Peninsula. The terrain is rugged in the inland part of the territory, and the highest peaks are located close to the north-eastern border of the Community, forming part of the Iberian Mountain Range.

### 2.3 The chilling hours correction

A method to carry out the topographic correction of chilling hours interpolation was developed. As in the case of the *topographic correction*, this method is executed only if the user uploads a DEM. Since the value of chilling hours is expressed as a count per station and not as a directly observed value by the weather station itself, as occurs for Tair, the topographic correction using Eq. (1) cannot be applied to correct the chilling hours interpolation. However, because the chilling hours

accumulation depends on air temperature, its interpolation without considering the elevation changes would imply an inaccurate estimate. In fact, considering the decreasing of temperature caused by higher elevations, in the same way the number of chilling hours should rise. For this reason, it was necessary to find a correction factor to obtain a more reliable evaluation of chilling hours within the study area.

The first step of this process was to consider 26 weather stations for calibration, and the remaining 15 for validation. The calibration stations were used to execute the interpolation (IDW) of the chilling hours, then the validation stations were used to extract the value to the points and compare the interpolated values to the observed ones within the pixels where the validation stations were located. The correction factor was identified considering the relationship between the *DEM.diff* (Eq. (2)) and the chilling hours difference (*Chill.diff*):

$$Chill.diff = Chill.int - Chill.obs \quad (3)$$

Where *Chill.int* represents the interpolated chilling hours, obtained with the calibration stations, and *Chill.obs* is the observed value of chilling hours, calculated as a cumulative sum per hydrological year for each validation station. The relationship between the value of *DEM.diff* detected for each validation stations using the DEM of Valencian Community and the average *Chill.diff* of the same station through all the years of weather data was evaluated through a quadratic function.

The proposed method was assessed using coefficient of determination ( $R^2$ ) and root mean squared error (RMSE, Eq. (4)).

$$RMSE = \sqrt{\frac{\sum_{i=1}^n (S_i - M_i)^2}{n}} \quad (4)$$

### 3. Results

Once the processing is completed, the user can visualize on canvas the principal outputs and, optionally, the selected additional outputs. Besides, the files that are stored inside the working

directory include the final map, the additional output(s) file(s) (if selected), the dataframe used for the interpolation process, and the provisional suitability layers for each year of data uploaded. Each visual output is uploaded on canvas automatically with a specific symbology.

### 3.1. The primary output types

Considering the reclassified maps (Figure 6c and 6d), the test case results are shown in Table 4. It appears that nearly the 70% of agricultural areas (according to CLC 2018, Figure 6d) results as unsuitable for avocado cultivation from Suitabox processing. The suitable and highly suitable areas are located in proximity of the coastal line and, particularly, in the south-eastern zone of the Community. The acreage of the suitability classes is reduced switching from the Reclassified map output to the one which considers the CLC, because the last one leaves out certain portions of land that are not used for agriculture. In fact, a large area of the Community (about the 60%) is reported as non-agricultural by CLC 2018.

*Table 4. The acreage of the different classes as resulted from the avocado test case, considering the Reclassified map (Figure 6c) and the Reclassified map with CLC (Figure 6d)*

<b>Output</b>	<b>Excluded areas (km<sup>2</sup>)</b>	<b>Unsuitable (km<sup>2</sup>)</b>	<b>Marginally suitable (km<sup>2</sup>)</b>	<b>Suitable (km<sup>2</sup>)</b>	<b>Highly suitable (km<sup>2</sup>)</b>
<b>Reclassified map</b>	0	18,724.32	1,592.17	2,187.25	758.3
<b>Reclassified map with CLC</b>	14,220.47	6,294.69	967.01	1,413.71	350.12

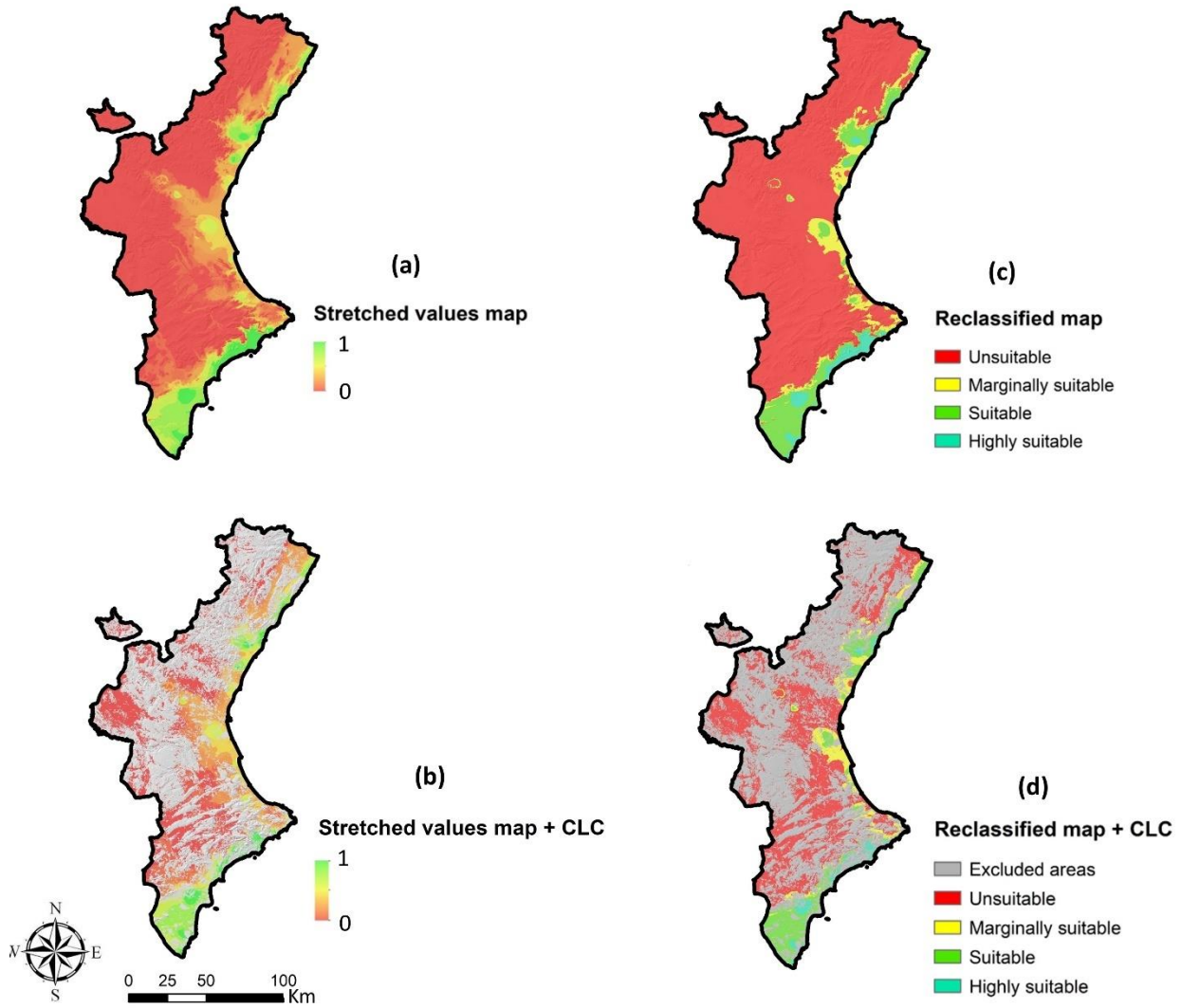


**Figure 6.** The different output types of the Crop Suitability tool resulted from the test case. In the Stretched values map with CORINE land cover (CLC) (b), the excluded areas are cut off from the layer, rather in the Reclassified map with CLC (d), the same areas are reclassified with a value of 0 (label: “Excluded areas”).

### 3.2. The additional outputs

Figure 7a shows the standard deviation map (SD map) obtained with the 5 years’ dataset applied in this case, while Figure 7b displays the uncertainty map derived from the weather stations’ location. The average value of the SD map obtained is 0.08, while the highest value is 0.47. Despite the maximum value, the average value is fairly low due to the fact that the majority of the study area does not show variation in the pixel value through the years considered in the test case. In fact, all the inland portion of the Valencian Community, which in the main output resulted as unsuitable for avocado, has a standard deviation value of 0 or nearly close to it, despite a few spots. The highest

values of standard deviation are concentrated along the coastline and the southern area, while the only portion of land which was classified as highly suitable in Figure 6c and 6d displays a standard deviation equal to 0.

The uncertainty map is computed considering an interval range of 10 km among the symbology classes, but the user can simply and manually customize this range (by manipulating the layer's symbology) depending on the necessities. This map shows with a color ramp, switching from deep green to deep red, the locations where the output should be more reliable because of the proximity to the weather stations. The acreage resulting inside the 10 km buffer is equal to 8092.35 km<sup>2</sup>, nearly 35% of the entire area of the Valencian Community, representing the most important class (in terms of surface acreage) among the buffer zones (Table 5).

*Table 5. The buffer zone of the uncertainty map (Figure 7b) and related acreages.*

<b>Buffer zone (km)</b>	<b>Acreage (km<sup>2</sup>)</b>
0 – 10	8092.35
10 – 20	8032.22
20 – 30	3817.72
30 – 40	1978.48
40 – 50	772.58
50 – 60	398.29
60 – 70	159.26
70 – 80	14.91



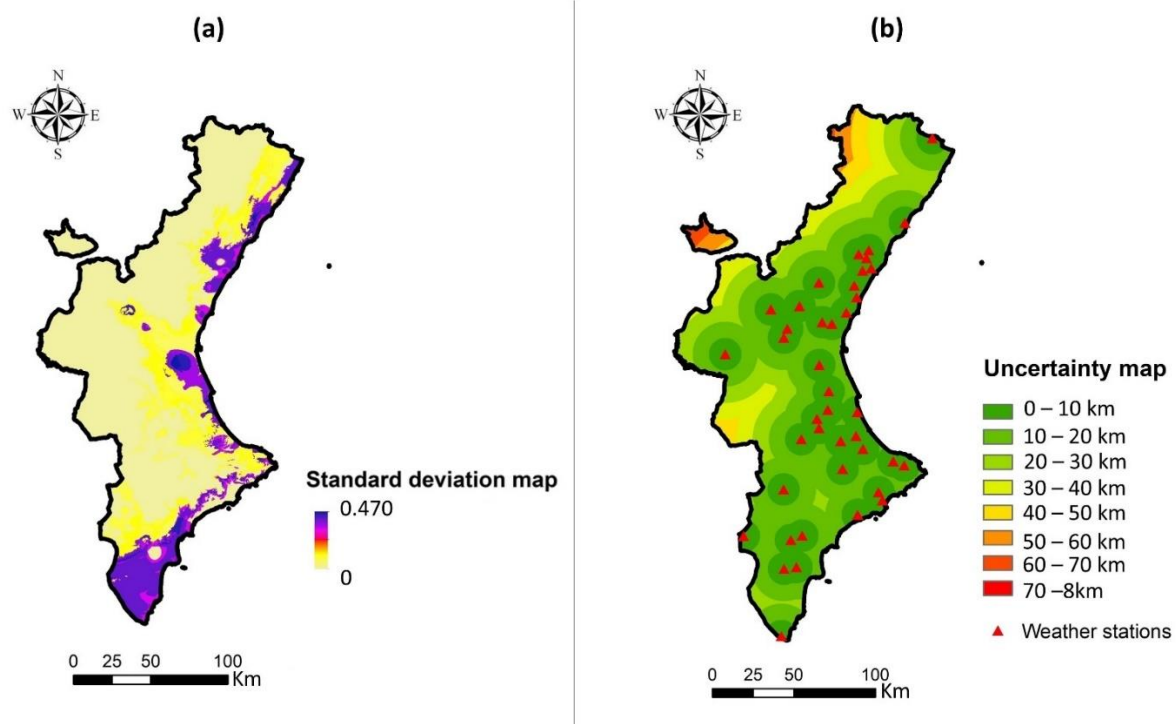


**Figure 7.** The additional outputs of the Crop Suitability tool. The Uncertainty map symbology is classified with 10 km of range, but the user can manually modify this range.

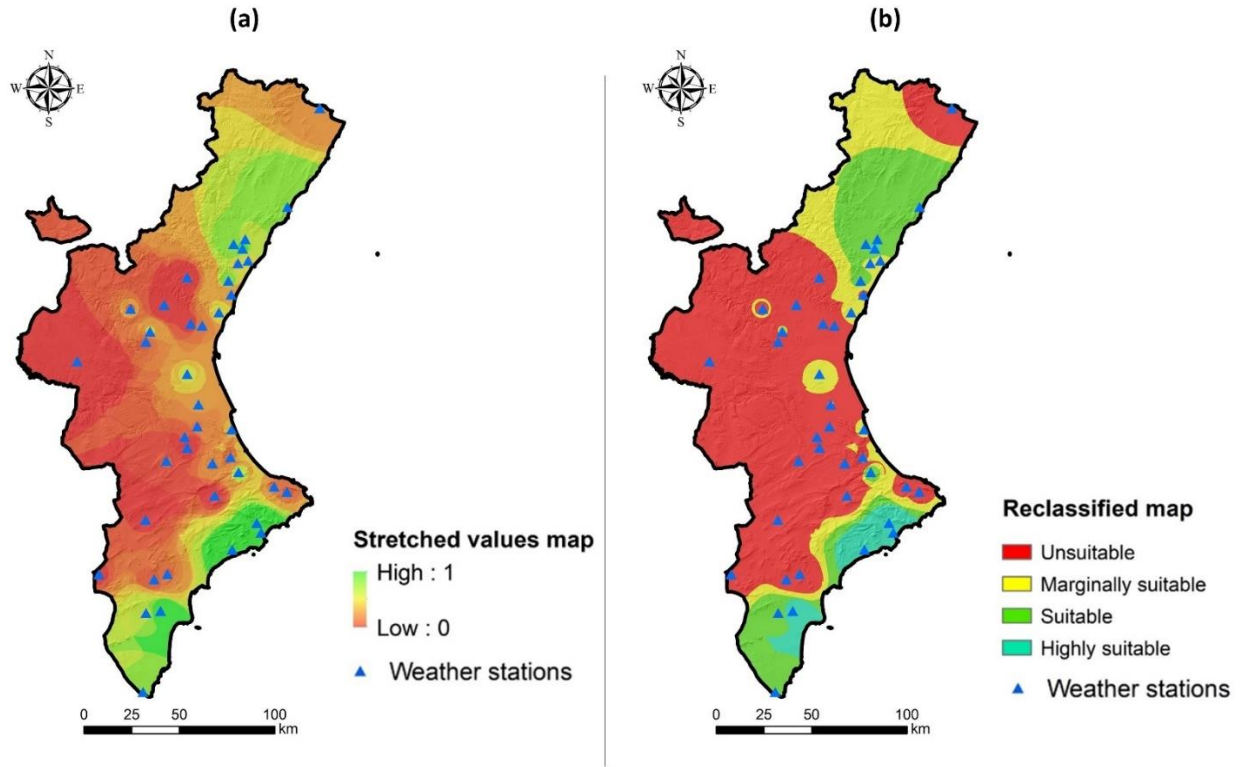
### 3.2. The topographic correction

Figure 8a and b show the stretched values and the reclassified maps, respectively, obtained without using the *topography correction* option. Besides the negative aesthetic effect, the non-utilization of the *topographic correction* causes acreage discrepancies among the 4 classes of the reclassified map. Considering this last output type, a comparison between the result obtained using the *topographic correction* (Figure 6c) and the one obtained without correction (Figure 8b) was carried out. The differences in the classes' acreage of these two outputs are reported in Table 6. In this analysis, the reclassified map without CLC areas has been considered in order to provide a more meaningful output from a visual point of view. The values in Table 6 show that, regarding the unsuitable class, the acreage has decreased of 4,621.36 km<sup>2</sup> passing from the topography-corrected output to the uncorrected one, since the terrain elevation (and its effect on temperature) is not taken into consideration during the processing. Indeed, the northern-internal part of the study area is reported as suitable in Figure 8b, despite the fact it is characterized of higher altitudes. On the other hand, the

acreage of the other classes has increased in the uncorrected output, especially the marginally suitable class, which has more than doubled (from 1,592.17 to 3,905.52 km<sup>2</sup>).

*Table 6. Different classes' acreage (km<sup>2</sup>) obtained with the utilization of the topography correction option. In brackets are shown the values related to the map considered the CLC areas.*

<b>Class</b>	<b>Acreage with correction (km<sup>2</sup>)</b>	<b>Acreage without correction (km<sup>2</sup>)</b>	<b>Difference (km<sup>2</sup>)</b>
<b>Unsuitable</b>	18,724.32 (6,294.69)	14,102.96 (5,712.08)	+4,621.36 (+582.61)
<b>Marginally suitable</b>	1,592.17 (967.01)	3,905.52 (1,119.40)	-2,313.35 (-152.39)
<b>Suitable</b>	2,187.25 (1,413.71)	4,045.73 (1,693.82)	-1,858.48 (-280.11)
<b>Highly suitable</b>	758.30 (350.12)	1,211.60 (500.94)	-453.30 (-150.82)



**Figure 8.** Stretched values map and reclassified map obtained without using the topography correction option.

### 3.4. Climate change projections

The plots in Figure 9 show the acreage (expressed in  $\text{km}^2$ ) of the reclassified map's 4 classes predicted by the two RCP scenarios considered in the test case, RCP 2.6 (Figure 9a) and RCP 8.5 (Figure 9b) according to the 4 different periods available (2020-2039, 2040-2059, 2060-2079, 2080-2099). The goal is to point out the discrepancies between the best- and the worst-case scenario.

As shown in the bar plots, according to RCP 2.6 the unsuitable areas tend to decrease from the current status ( $18,724.32 \text{ km}^2$ ) to the temporarily farther period, i.e., 2080-2099 ( $17,331.59 \text{ km}^2$ ). Besides, according to the most severe scenario (RCP 8.5), the same class shows a relevant reduction until the 2040-2059 period ( $16,521.39 \text{ km}^2$ ), and subsequently it starts to rise again until reaching  $17,936.41 \text{ km}^2$  in the period 2080-2099. On the contrary, considering RCP 8.5, the highly suitable class displays an increase until 2040-2059, when it reaches  $1,415.90 \text{ km}^2$ , after which it starts to fall until a value ( $508.81 \text{ km}^2$ ) lower than the current situation ( $758.30 \text{ km}^2$ ). The same class is defined by a different

behavior in RCP 2.6 scenario, where it rises continuously to 1,282.12 km<sup>2</sup>. The suitability class also increases regularly according to RCP 2.6, realizing 3,283.27 km<sup>2</sup>, whilst in RCP 8.5 it shows the first increase in 2020-2039, reaching 3,244.63 km<sup>2</sup>, then it falls to 1,748.99 km<sup>2</sup> in 2080-2099. Lastly, the marginally suitable class is characterized by a smooth and low reduction up to 1,365.06 km<sup>2</sup> considering RCP 2.6, though it has a tortuous evolution in the RCP 8.5 scenario: it shows a first reduction in 2020-2039 down to 1,340.85 km<sup>2</sup>, afterward it increases in 2040-2059 and 2060-2079 km<sup>2</sup> up to 3183.63 km<sup>2</sup>, then it has a final and low reduction to 3067.83 km<sup>2</sup> in 2080-2099. The readers are referred to the Supplementary material section (Figure S1 and S2) for the visualization of the resulting maps for each RCP and period considered.

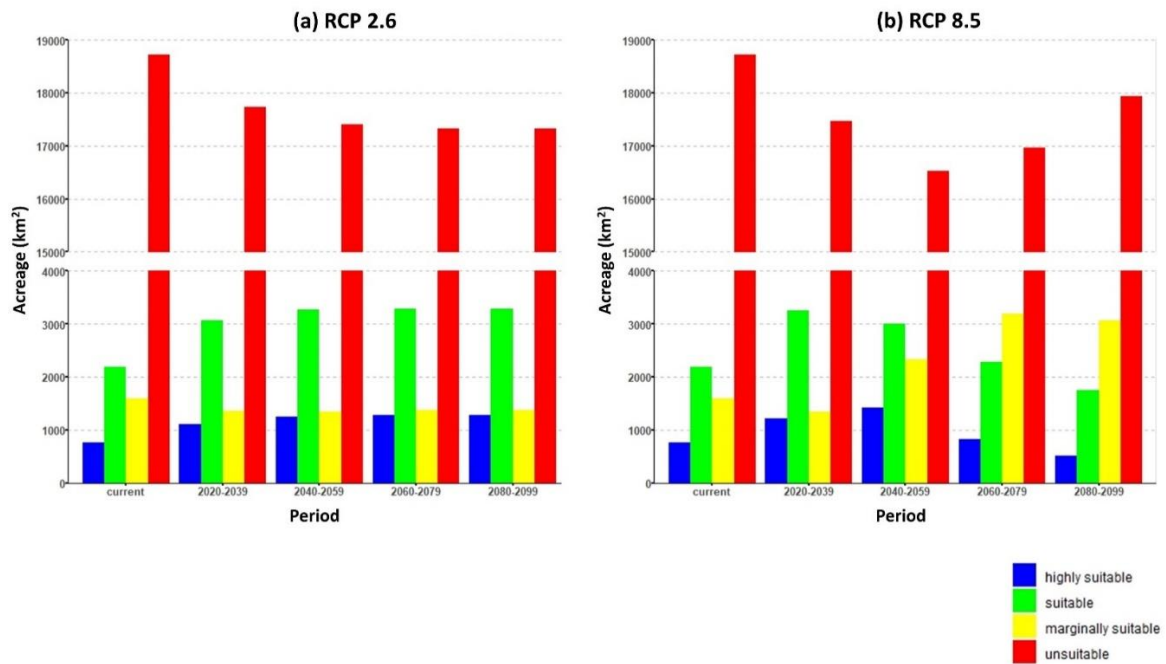


**Figure 9.** Differences in the acreage of the 4 classes expected by RCP 2.6 and RCP 8.5 for the avocado test case.

### 3.5 Application of the chilling hours correction

Figure 10 shows the relationship between *DEM.diff* (Eq. (2)) and *Chill.diff* (Eq. (3)) described by a polynomial function of degree 2, obtaining  $R^2 = 0.66$ . The chilling hours correction is executed as follows:

$$Chill.corr = Chill.int - (-0.0032 * (DEM.diff)^2) \quad (4)$$

where *Chill.corr* is the corrected number of chilling hours per pixel of the interpolated raster layer. Without using this correction, a RMSE value of 301 was obtained comparing the interpolated chilling hours using the calibration stations and observed values of the validation stations, while using the correction factor this value decreased to 218, obtaining a lower error.

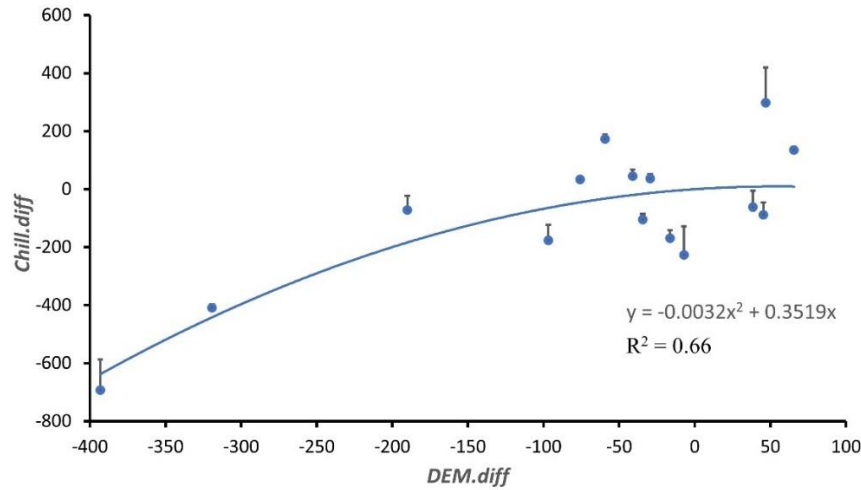


**Figure 10.** Relationship between *DEM.diff* and *Chill.diff*.

The proposed method was applied using kiwifruit (cultivar: Jinyan) to show the significant differences derived from its use. Figure 11 shows the (reclassified) maps obtained without using the chilling hour correction (Figure 11a) and with the proposed method implemented (Figure 11b). It can be noted that in 11b there is a higher distribution of suitable and marginally suitable areas, depending on the better connection between terrain elevation and chilling hours accumulation. In fact, these areas are located in proximity of hills and mountains, hence where the altitude is greater, resulting in lower extent of unsuitable areas compared to 11a. Furthermore, some artifacts around a few weather

stations are displayed in 11a, due to the fact that the interpolation of chilling hours was incoherent with terrain altitude alteration.

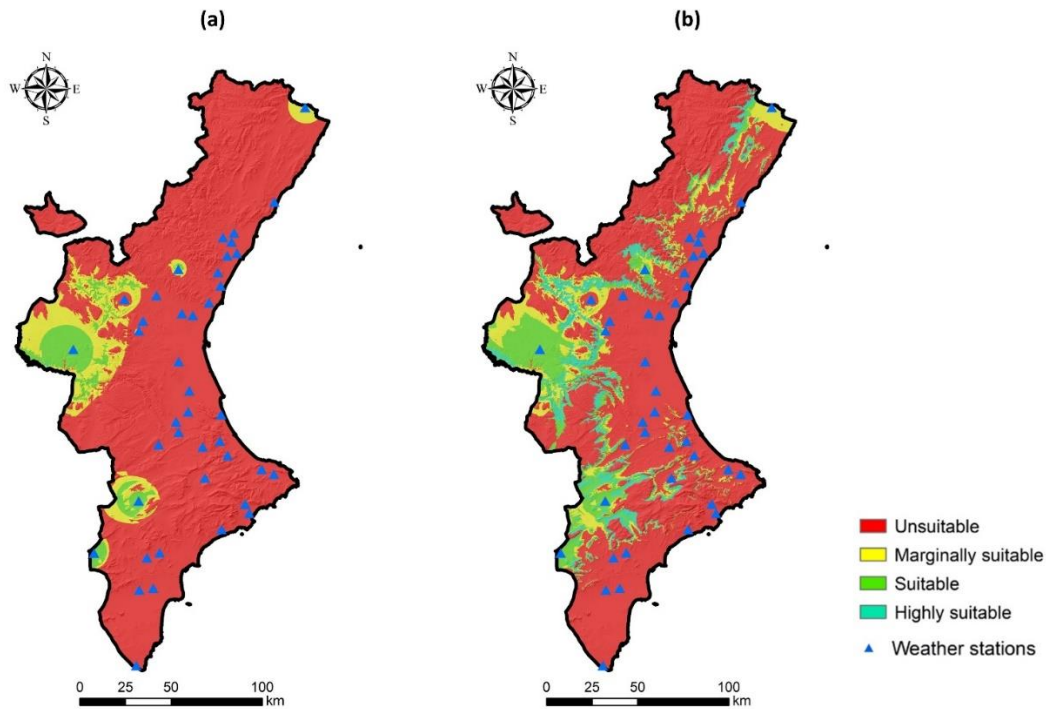


**Figure 11.** Resulting (reclassified) maps considering kiwifruit (cultivar: Jinyan) without chilling hours correction (a) and with the application of the proposed correction method (b).

#### 4. Discussion

Suitabox has the capability to add value to studies on suitability analysis related to a specific crop for a certain area and the evaluation of climate change's effects on crops' suitability distribution. For instance, it is shown in Figure 6, the most important part of highly suitable areas for avocado cultivation are located close to the south-eastern coast (nearby the towns of Callosa d'en Sarrià and Altea) which is, at this time, the most important area of avocado production in the Valencian Community. Also, the map indicates that the unsuitable areas are represented by the most-internal zone of the region, which is predominantly hilly and mountainous, pointing out how temperature affects avocado growing and flowering (Lahav and Trochoulis, 1982; Sedgley, 1977). Also, the suitable and highly suitable areas displayed on the north-eastern coast (near the towns of Castellon

and Villareal), which is an area where avocado cultivation currently exists but does not fill all the extension shown on the map, are an interesting insight for future research. In fact, currently there are about 20 km<sup>2</sup> of avocado orchards in Valencian Community, mainly concentrated in the above-mentioned area (south-eastern zone of the region). However, Suitabox's findings (Figure 6d) reveals that there is 1763,83 km<sup>2</sup> of potential useable acreage for avocado cultivation, based on the suitable and highly suitable classes, implying that only around 1.13% of the Valencian Community's capability is dedicated to this crop. It suggests that, despite the fact that our study region is the second-largest Autonomous Community for avocado production (after Andalusia), there may be significant untapped potential. Indeed, there are other factors that influence crop distribution, but our study did not attempt to describe in detail the reality of a tree crop's climate appropriateness, which is a complex theme and would require more years of agrometeorological datasets, as well as types of data. In addition, the results of this toolbox may be improved in quality and reliability through more specific agroecological parameters related to the considered crop species, pointing out that it is still difficult to identify clear thresholds in the scientific literature today.

To the best of our knowledge there is not an ArcGIS toolbox that automate this kind of process, being executed with the support of conventional GIS tools in a slower way. Indeed, the major potentiality of Suitabox lies in the fact that it can be included in a more in-depth study, such as the suitability assessment works mentioned in the introduction, where the authors used multi-criteria decision analysis (MCDA) considering also agroecological parameters of the analyzed crops related to the weather. The proposed toolbox has the capacity to boost these studies, speeding up the phase concerning the weather variables.

Another potential utility of Suitabox is to help in decision making processes for agricultural policy and planning. Agricultural land use planning is crucial to avoid problems related to land degradation and overexploitation of natural resources. In fact, as stated by FAO in 1976, 1983 and 2007, the last

decades of agricultural land usage have resulted in much more devastation than returning of resources, due to a lack of concern about the appropriateness of the land for specific activities or crops.

Concerning the additional outputs of Suitabox (Figure 7), the obtained SD map (Figure 7a) displays that in the most-internal mountainous areas the standard deviation is small (close to or equal to 0), pointing out that in such zones the pixel score is always very low, due to the too low temperatures for avocado plants. The adverse relation between avocado and low temperature was confirmed in the past from several studies of Sedgley and co-authors (1977, 1981, 1983), reporting that low temperatures (12-17 °C) caused the inhibition of pollen tube growth, and the typical female opening and male anthesis were considerably delayed. Because of the cold temperature, there was little or no flower fertilization resulting in failures in fruit set. On the other hand, the uncertainty map (Figure 7b) was useful to display the areas where the reliability of the map differs, showing in green the zones which are closer to the weather stations. As a result, the output obtained in the Valencian Community's internal zones appear to be less credible, owing to a lack of weather stations in those areas, which are associated with higher elevations and slopes, as well as the absence of irrigated farmland. Mourtzinis et al. (2016) highlighted the importance of weather station density in agricultural regions, demonstrating that a denser station network results to a more reliable interpolation of measured weather data (MWD). However, SiAR network may not be considered a low-density network, since there is one station per 567 km<sup>2</sup> (considering the 41 stations used in this work), but it is characterized by a non-uniform distribution on the whole territory.

In relation to the *topographic correction* option of the Crop Suitability tool, Figures 8a and 8b show that without the use of a DEM in the processing the tool returns a map with an artifact commonly called “bull’s eye” (Gotway et al., 1996). This is a typical effect of the IDW interpolation method, which produces isolated circles and concentric circles around known measured points (in this case, the weather stations), affecting the aesthetic property and accuracy of the map (Li et al., 2018). The obtained results are particularly relevant, and emphasize the significance of this correction, for the



northern area of the Valencian Community, where Figure 8b shows a big and circle suitable zone, while in Figure 6 the same area is reported as unsuitable (or is excluded according to CLC).

Finally, the last feature of Suitabox tested in this study case was the possibility to implement a climate change projection. While there are several studies emphasizing the relevant influence of air temperature on avocado physiology during flowering and fruit set (Sedgley, 1977; Sedgley and Annels, 1981; Sedgley and Grant, 1983; Pattemore et al., 2018), Howden et al. (2005) stated that climate change could feasibly affect the avocado industry in many ways. The particular behavior of RCP 8.5 is because this model leads to a more impactful temperature raise, causing a decline in unsuitable areas, while the highly suitable areas increase by the 86% until 2040-2059; after this period the temperature raise becomes harmful for avocados, exceeding the temperature threshold during the fruit growth, which turns into a dangerous condition for this phenology step (Table S1).

The strengths and limitations of Suitabox are illustrated hereafter:

- It is able to spatialize crops' ecological factors related to air temperature using IDW. However, the availability of different approach (e.g., geostatistical methods, such as kriging) would enhance the toolbox usefulness;
- The modular structure of Suitabox allows to include new meteorological variables for different crop species, thanks to the combination of the *Custom Crop Pre-processing* tool and the *Custom crop* option in the Crop Suitability tool. However, a greater number of function (currently six), combined with the implementation of different meteorological variables, would improve the value of this features
- It allows the use of agrometeorological datasets of different length. Potentially there is no limit to the number of datasets that the user can upload in the Crop Suitability tool.
- It provides easy and friendly outputs, especially regarding the reclassified map (Figure 6) because categorizes the different areas, providing a more insightful map.

- The inclusion of CORINE land cover allows to exclude specific areas (urban, forestry, water bodies, etc.), obtaining a more insightful output which considers only agricultural lands and returning a more accurate acreage of the different classes. Nevertheless, since CLC covers only European areas, the possibility to upload a different land use layer and with different map scale would surely be useful for studies based in every part of the world.
- It can perform the topographic correction of interpolated temperatures and chilling hours. However, the latest method has been developed considering topographic data of our study area (i.e., the DEM of Valencian Community), therefore it would be insightful to test this method in different territories to evaluate its performance, or to elaborate an approach equally applicable to any area able to reduce more the error.
- It is able to consider the intra-pixel variability in terms of different agrometeorological years and the distance to the closes weather station, thanks to the additional output;
- Suitabox includes the possibility to implement a climate change scenario, choosing an RCP model. This feature is significant considering the impacts of climate changes on agriculture, forcing the farmers to respond to these changes, particularly in terms of modifying the timing of cultivation and choosing different crops and cultivars (Olesen et al., 2011).
- Suitabox can be downloaded easily and freely from its GitHub repository (<https://github.com/96francesco/suitabox>) and it will remain an open-source project, with the goal to stimulate a collaboration with who will be intrigued by this work, trying to release subsequent and upgraded versions of the software and taking advantage of all the positive mechanisms that this kind of cooperation and platform like GitHub bring (Dabbish et al., 2012).

## **5. Conclusions**

In this study, a novel ArcGIS toolbox for crops' suitability and site selection based on weather data was developed and tested in a Mediterranean environment (Valencian Community, Spain). Suitabox has the potential to be used in a variety of studies, from multi-criteria decision analysis for crop suitability assessment to climate change consequences on existing crop suitability in a specific site. Furthermore, the research of alternative crops to stimulate local agricultural activities, as well as trends determining the diffusion of unconventional species in a given region, frequently results in economic failures and natural resources damage. In such situations, it would be prudent for local authorities and stakeholders to perform some research to assess the new crop's potential success or, at least, its suitability related to local environmental and socio-economic factors (e.g., weather, pedology, infrastructure, etc.). Suitabox might easily fit into this framework, providing policymakers with a simple tool that, when complemented with other instruments and expertise, can help support these research. Suitabox is undoubtedly hampered by various limitations, including a scarcity of precise information regarding crop ecological requirements that can be used for this type of activity in the literature. The goal of this project was to provide a simple tool that researchers, policymakers, GIS technicians, and inexperienced users could use to make better agricultural planning and crop management decisions while pursuing a more sustainable use of natural resources. Another major goal is to encourage the developer community to participate in this project by testing the software and providing feedback on how Suitabox may be improved. Developers are encouraged to download the program from the online repository, test it, and contribute to the codebase via pull requests, issues or forks. Future software updates will almost certainly be required to address the aforementioned constraint and increase the trustworthiness of the results.

## References

- Alcaraz Arco M. L., 2009. Biología Reproductiva del Aguacate (*Persea americana* Mill.). Implicaciones Para la Optimización del Cuajado. Doctoral dissertation (in Spanish). Universidad de Malaga, Facultad de Ciencias – Departamento de Microbiología.
- Allaw K. and Al-Shami L., 2018. Geographic Information System-Based Map for Agricultural Management in South-Lebanon. 2018 International Arab Conference on Information Technology (ACIT). Year: 2018, Volume: 1, Pages: 1-11. DOI: 10.1109/ACIT.2018.8672702
- Amman C., Boehnert, J., and Wilhelmi, O. 2018. “World Climate Data CMIP5 Multi Model Ensemble”. Research Applications Laboratory, National Center for Atmospheric Research, Boulder, Colorado. Obtained online 07 Jan 2022 at <https://learn.arcgis.com/en/projects/explore-future-climate-projections/>.
- Aslamarz, A.A., Vahdati, K., Rahemi, M., Hassani, D., 2009. Estimation of Chilling and Heat Requirements of Some Persian Walnut Cultivars and Genotypes. *HORTSCIENCE* 44(3):697–701.
- Barry, R.G. and Chorley, R.J. 1987. *Atmosphere, Weather and Climate*, 5<sup>th</sup> edn. Methuen, London and New York, 460 pp
- Chen, FW., Liu, CW. Estimation of the spatial rainfall distribution using inverse distance weighting (IDW) in the middle of Taiwan. *Paddy Water Environ* 10, 209–222 (2012). <https://doi.org/10.1007/s10333-012-0319-1>
- Dabbish, L., Stuart, C., Tsay, J., & Herbsleb, J. (2012). Social coding in GitHub. *Proceedings of the ACM 2012 Conference on Computer Supported Cooperative Work - CSCW '12*. doi:10.1145/2145204.2145396
- Dubrovina, I.A., Bautista, F., 2014. Analysis of the Suitability of Various Soil Groups and Types of Climate for Avocado Growing in the State of Michoacan, Mexico. ISSN 1064\_2293, *Eurasian Soil Science*, 2014, Vol. 47, No. 5, pp. 491–503. © Pleiades Publishing, Ltd., 2014. DOI: 10.1134/S1064229314010037

- European Union, Copernicus Land Monitoring Service 2022, European Environment Agency (EEA)
- FAO, 1976. A framework for land evaluation. Food and Agriculture Organization of the United Nations, Soils Bulletin 32. FAO, Rome.
- FAO, 1983. Guidelines: land evaluation for rainfed agriculture. Food and Agriculture Organization of the United Nations, Soils Bulletin 52. Rome, Italy.
- FAO, 1996. Agro-Ecological Zoning Guidelines. FAO Soils Bulletin 73, Rome < <http://www.fao.org/3/w2962e/w2962e00.htm> > (accessed 05 Oct 2021)
- FAO, 2007. Land Evaluation: Towards a Revised Framework. FAO, Rome.
- Gotway, C. A., Ferguson, R. B., Hergert, G. W., & Peterson, T. A. (1996). Comparison of Kriging and Inverse-Distance Methods for Mapping Soil Parameters. Soil Science Society of America Journal, 60(4), 1237. doi:10.2136/sssaj1996.03615995006000040040x
- Hatfield, J. L., & Prueger, J. H. (2015). Temperature extremes: Effect on plant growth and development. Weather and Climate Extremes, 10, 4–10. Doi:10.1016/j.wace.2015.08.001
- Hewett, E.W., Young, K. 1981. Critical freeze damage temperatures of flower buds of kiwifruit (*Actinidia chinensis* Planch.), New Zealand Journal of Agricultural Research, 24:1, 73-75, DOI: 10.1080/00288233.1981.10420873
- Ijaz M., Nawaz A., Ul-Allah S., Rizwan M. S., Ullah A, Hussain M., Sher A., Ahmad S., 2019. Crop Production Under Changing Climate: Past, Present and Future, in: Hasanuzzaman M. (Ed), Agronomic Crops, Volume 1: Production Technologies, Springer Nature Singapore Pte Ltd, pp. 149 – 173. DOI: <https://doi.org/10.1007/978-981-32-9151-5>
- IPCC (Intergovernmental Panel on Climate Change). 2013. Climate change 2013: The physical science basis. Working Group I contribution to the IPCC Fifth Assessment Report. Cambridge, United Kingdom: Cambridge University Press.
- IPCC (Intergovernmental Panel on Climate Change). 2014: Climate Change 2014: Synthesis Report. Contribution of Working Groups I, II and III to the Fifth Assessment Report of the

- Intergovernmental Panel on Climate Change [Core Writing Team, R.K. Pachauri and L.A. Meyer (eds.)]. IPCC, Geneva, Switzerland, 151 pp.
- Iizumi, T., Ramankutty, N. How do weather and climate influence cropping area and intensity?, *Global Food Security*, Volume 4, 2015, Pages 46-50, ISSN 2211-9124, <https://doi.org/10.1016/j.gfs.2014.11.003>.
- Jha, P.K., Materia, S., Zizzi, G., Costa-Saura, J.M., Trabucco, A., Evans, J., Bregaglio, S., 2020. Climate change impacts on phenology and yield of hazelnut in Australia, *Agricultural Systems*, Volume 186, 2021, 102982, ISSN 0308-521X, <https://doi.org/10.1016/j.agsy.2020.102982>.
- Lahav, E., and Trochoulis, T. (1982). The effect of temperature on growth and dry matter production of avocado plants. *Australian Journal of Agricultural Research*, 33(3), 549. <https://doi.org/10.1071/AR9820549>
- Ledley, T. S., Sundquist, E. T., Schwartz, S. E., Hall, D. K., Fellows, J. D., & Killeen, T. L. (1999). Climate change and greenhouse gases. *Eos, Transactions American Geophysical Union*, 80(39), 453–458. Doi:10.1029/99eo00325
- Li, J., Heap, A.D., 2008. A Review of Spatial Interpolation Methods for Environmental Scientists. *Geoscience Australia, Record 2008/23*, 137 pp.
- Li, J., Heap, A.D., 2011. A review of comparative studies of spatial interpolation methods in environmental sciences: performance and impact factors. *Ecol.Inform.* 6, 228–241. <https://doi.org/10.1016/j.ecoinf.2010.12.003>
- Li, Z., Wang, K., Ma, H., Wu, Y. (2018). An Adjusted Inverse Distance Weighted Spatial Interpolation Method. *Advances in Computer Science Research*, volume 65. 3<sup>rd</sup> International Conference on Communications, Information Management and Network Security (CIMNS 2018).
- Lu, G. Y., & Wong, D. W. (2008). An adaptive inverse-distance weighting spatial interpolation technique. *Computers & Geosciences*, 34(9), 1044–1055. <https://doi.org/10.1016/j.cageo.2007.07.010>

- Malone, B.P., Kidd, D.B., Minasny, B., McBratney, A.B., 2015. Taking account of uncertainties in digital land suitability assessment. *PeerJ* 3:e1366; DOI 10.7717/peerj.1366
- Manabe, S. (2019) Role of greenhouse gas in climate change, *Tellus A: Dynamic Meteorology and Oceanography*, 71:1, DOI: 10.1080/16000870.2019.1620078
- McGranahan, G., Leslie, C., Bujazha, D., Manterola, N., Hirbod, S., Dandekar, A., Aradhya, M., Beede, B., Olson, B., Anderson, K.K., Grant, J., Britton, M., Caprile, J., Coates, B. 2006. WALNUT IMPROVEMENT PROGRAM 2006. Walnut Research Reports. URL: [http://walnutresearch.ucdavis.edu/Topic\\_results.asp?txtSecNo=2](http://walnutresearch.ucdavis.edu/Topic_results.asp?txtSecNo=2)
- Mehlenbacher, S.A., 1991. Chilling requirements of hazelnut cultivars. *Scientia Hort.*, 47:271-282
- Ministerio de Agricultura, Pesca y Alimentación (MAPA), 2020, Estadísticas agrarias. <<https://www.mapa.gob.es/es/estadistica/temas/default.aspx>> (accessed 22/03/2022)
- Moeletsi, M. E., Shabalala, Z. P., De Nysschen, G., and Walker, S. (2016). Evaluation of an inverse distance weighting method for patching daily and decadal rainfall over the Free State Province, South Africa. *Water SA*, 42(3), 466-474. <https://dx.doi.org/10.4314/wsa.v42i3.12>
- Mourtzinis, S., Rattalino Edreira, J. I., Conley, S. P., & Grassini, P. (2017). From grid to field: Assessing quality of gridded weather data for agricultural applications. *European Journal of Agronomy*, 82, 163–172. doi:10.1016/j.eja.2016.10.013
- Namesny, A., Conesa, C., Hormaza, I., Lobo, G., 2020. Cultivo, poscosecha y procesado del aguacate. Valencia, Spain
- Noti, V., 2014. GIS open source per geologia e ambiente (in Italian), Dario Flaccovio Editore s.r.l., Palermo (Italy)
- Olesen, J. E., Trnka, M., Kersebaum, K. C., Skjelvåg, A. O., Seguin, B., Peltonen-Sainio, P., , Rossi, F., Kozyra, J., Micale, F. (2011). Impacts and adaptation of European crop production systems to climate change. *European Journal of Agronomy*, 34(2), 96–112. doi:10.1016/j.eja.2010.11.003

- Pattemore, D. E., Buxton, M. N., Cutting, B. T., McBrydie, H. M., Goodwin, R. M., & Dag, A. (2018). Low overnight temperatures delay ‘Hass’ avocado (*Persea americana*) female flower opening, leading to nocturnal flowering. *Journal of Pollination Ecology*, 23, 127–135. [https://doi.org/10.26786/1920-7603\(2018\)12](https://doi.org/10.26786/1920-7603(2018)12)
- Ramankutty, N., Foley, J.A., Norman, J., Mcsweeney, K. 2002 Blackwell Science Ltd, *Global Ecology & Biogeography*, 11, 377–392. <https://doi.org/10.1046/j.1466-822x.2002.00294.x>
- Ramírez-Cuesta, J.M., Cruz-Blanco, M., Santos C., Lorite, I.J, 2017. Assessing reference evapotranspiration at regional scale based on remote sensing, weather forecast and GIS tools. *International Journal of Applied Earth Observation and Geoinformation* 55 (2017) 32–42. DOI: <http://dx.doi.org/10.1016/j.jag.2016.10.004>
- Ruiz-Corral J.A., Medina Garcia G., Gonzalez Acuña I.J., Flores H.E., Ramirez Ojeda G., *Requerimientos agroecológicos de cultivos 2da Edición*. Instituto Nacional de Investigaciones Forestales Agrícolas y Pecuarias (in Spanish). ISBN: 978-607-37-0188-4.
- Sedgley, M. (1977). The Effect of Temperature on Floral Behaviour, Pollen Tube Growth and Fruit Set in the Avocado. *Journal of Horticultural Science*, 52(1), 135–141. doi:10.1080/00221589.1977.1151473
- Sedgley, M., & Annells, C. M. (1981). Flowering and fruit-set response to temperature in the avocado cultivar “Hass.” *Scientia Horticulturae*, 14(1), 27–33. doi:10.1016/0304-4238(81)90075-3
- Sedgley, M., & Grant, W. J. R. (1983). Effect of low temperatures during flowering on floral cycle and pollen tube growth in nine avocado cultivars. *Scientia Horticulturae*, 18(3), 207–213. doi:10.1016/0304-4238(83)90023-7
- Selim S., Koc-San D., Selim C. and Taner San B., 2018. Site selection for avocado cultivation using GIS and multi-criteria decision analyses: Case study of Antalya, Turkey. *Computers and Electronics in Agriculture* 154 (2018) 450-459. <https://doi.org/10.1016/j.compag.2018.09.038>



- Tercan, E., Ali Dereli, M., 2020. Development of a land suitability model for citrus cultivation using GIS and multi-criteria assessment techniques in Antalya province of Turkey, *Ecological Indicators*, Volume 117, 2020, 106549, ISSN 1470-160X, <https://doi.org/10.1016/j.ecolind.2020.106549>.
- Vahdati, K., Massah Bavani, A.R., Khosh-Khui, M., Fakour, P., Sarikhani, S., 2019. Applying the AOGCM-AR5 models to the assessments of land suitability for walnut cultivation in response to climate change: A case study of Iran. *PLoS ONE* 14 (6): e0218725. <https://doi.org/10.1371/journal.pone.0218725>
- van Vuuren, D.P., Edmonds, J., Kainuma, M. et al. The representative concentration pathways: an overview. *Climatic Change* 109, 5 (2011). <https://doi.org/10.1007/s10584-011-0148-z>
- Wall, C., Dozier, W., Ebel, R. C., Wilkins, B., Woods, F., Foshee, W., III. (2008). Vegetative and Floral Chilling Requirements of Four New Kiwi Cultivars of *Actinidia chinensis* and *A. deliciosa*, *HortScience horts*, 43(3), 644-647. DOI: <https://doi.org/10.21273/HORTSCI.43.3.644>
- Wang, S., Huang, C., Tao, J., Zhong, M., Qu, X., Wu, H., Xu, X., 2017. Evaluation of chilling requirement of kiwifruit (*Actinidia* spp.) in south China, *New Zealand Journal of Crop and Horticultural Science*, DOI: 10.1080/01140671.2017.1334670
- Weinberger, J.H. Requirements of Peach Varieties. *Proc. Am. Soc. Hortic. Sci.* 1950, 56, 122–128.
- Woodward, F. I., & Williams, B. G. (1987). Climate and plant distribution at global and local scales. *Vegetatio*, 69(1-3), 189–197. doi:10.1007/bf00038700
- Zhao, T., Li, D., Li, L., Han, F., Liu, X., Zhang, P., Chen, M., & Zhong, C. (2017). The Differentiation of Chilling Requirements of Kiwifruit Cultivars Related to Ploidy Variation, *HortScience*, 52(12), 1676-1679. DOI: <https://doi.org/10.21273/HORTSCI12410-17>

Supplementary material

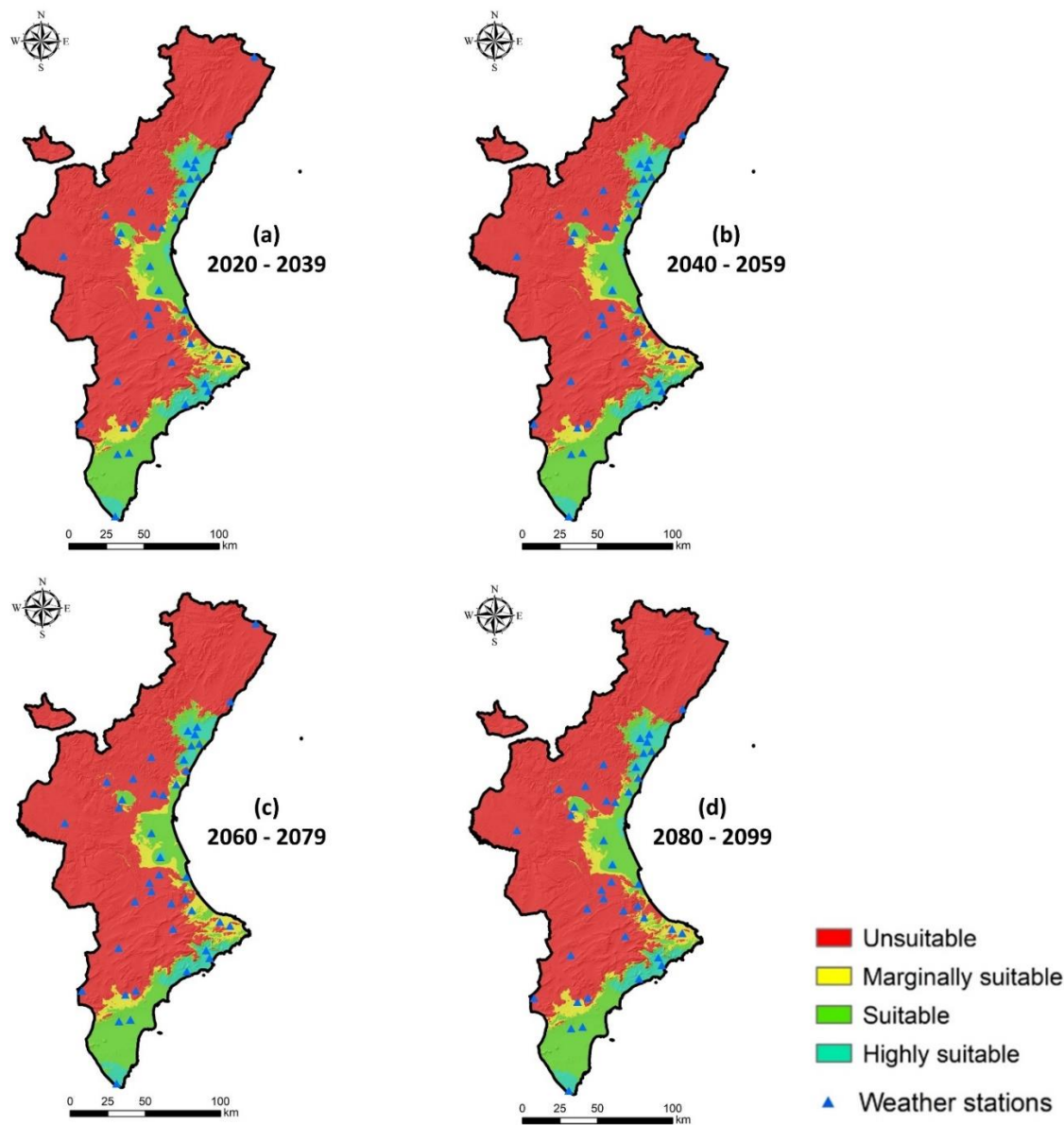


**Figure S1.** Reclassified maps resulted from the avocado test case, applying all the 4 available periods of RCP 2.6

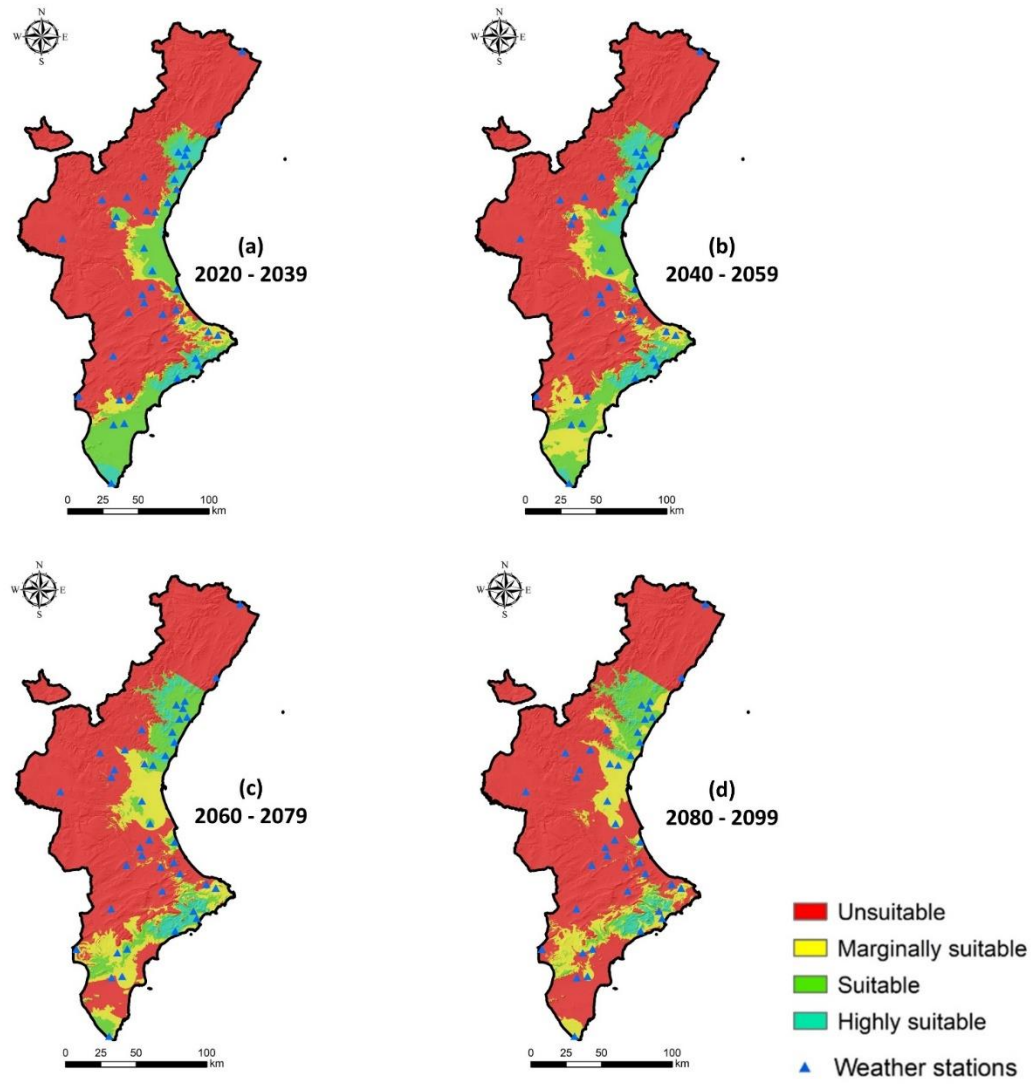


**Figure S2.** Reclassified maps resulted from the avocado test case, applying all the 4 available periods of RCP 8.5

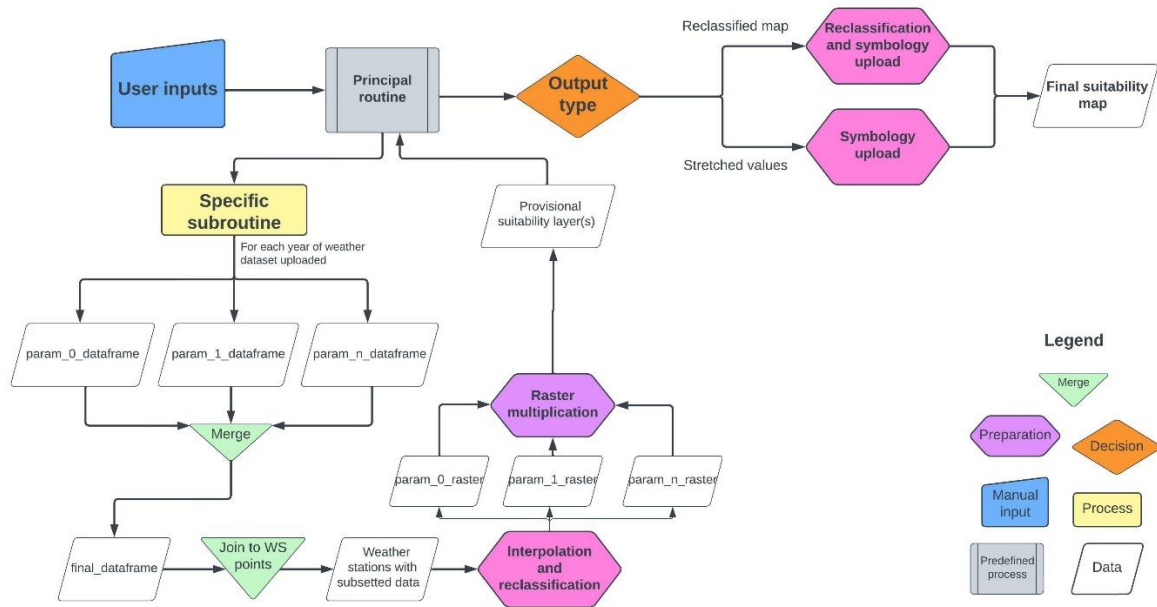


**Figure S3.** Core workflow of the Crop Suitability tool

**Table S1.** Crop's requirement table used for avocado. Each parameter considered can have 4 value ranges: unsuitable, marginally suitable, suitable, and highly suitable. Blank cells will not be considered

Parameter	Unsuitable	Marginally suitable	Suitable	Highly suitable	DoY range	Literature reference
Average annual temperature	$t < 12\text{ }^{\circ}\text{C}$	$12 \leq t \leq 15\text{ }^{\circ}\text{C}$		$t > 15\text{ }^{\circ}\text{C}$	1-365	Dubrovina and Bautista, 2014
Minimum temperature	$t \leq -2\text{ }^{\circ}\text{C}$		$-2 < t \leq 0\text{ }^{\circ}\text{C}$	$t > 0\text{ }^{\circ}\text{C}$	1-365	Ruiz-Corral et al., 2020
Average winter temperature	$t \leq 5\text{ }^{\circ}\text{C}$			$t > 5\text{ }^{\circ}\text{C}$	335-59	Namesny et al., 2020
Average maximum temperature during flowering	$t > 30\text{ }^{\circ}\text{C}$			$t \leq 30\text{ }^{\circ}\text{C}$	60-151	Alcaraz, 2009
Average temperature during flowering	$t < 10\text{ }^{\circ}\text{C}$ and $t > 35\text{ }^{\circ}\text{C}$			$10 \leq t \leq 35\text{ }^{\circ}\text{C}$	60-151	Selim et al., 2018
Maximum temperature during fruit set and growth	$t \geq 42\text{ }^{\circ}\text{C}$	$40 \leq t < 42\text{ }^{\circ}\text{C}$		$t < 40\text{ }^{\circ}\text{C}$	152-365	Ruiz-Corral et al., 2020

Table S2. Crop's requirement table used for kiwifruit (*Actinidia* sp.)

Parameter	Unsuitable	Marginally suitable	Suitable	Highly suitable	DoY range	Literature reference
Early frost	$t \leq -1\text{ }^{\circ}\text{C}$	$-1 \leq t \leq 0\text{ }^{\circ}\text{C}$		$t > 0\text{ }^{\circ}\text{C}$	274-320	Garcia Rubio et al., 2015
Late frost (damages to flower buds)	$t \leq -3\text{ }^{\circ}\text{C}$	$-3 < t \leq -2\text{ }^{\circ}\text{C}$	$-2 < t \leq -1\text{ }^{\circ}\text{C}$	$t > -1\text{ }^{\circ}\text{C}$	121-151	Hewett and Young, 1981
Late frost (damages to vegetation buds)	$t \leq -2\text{ }^{\circ}\text{C}$	$-2 < t \leq -1.5\text{ }^{\circ}\text{C}$	$-1.5 < t \leq 0\text{ }^{\circ}\text{C}$	$t > 0\text{ }^{\circ}\text{C}$	60 -151	Hewett and Young, 1981
Maximum tolerated temperature	$t > 40\text{ }^{\circ}\text{C}$		$t \leq 40\text{ }^{\circ}\text{C}$		1-365	Ruiz-Corral et al., 2020
Chilling hours (CH) for vegetative budbreak (cv Donghong)	$\text{CH} < 222$			$\text{CH} \geq 222$	274-46	Zhao et al., 2017
Chilling hours (CH) for floral emergence (cv Donghong)	$\text{CH} < 655$			$\text{CH} \geq 655$	274-46	Zhao et al., 2017
Chilling hours (CH) for vegetative budbreak (cv Jintao)	$\text{CH} < 776$			$\text{CH} \geq 776$	274-46	Zhao et al., 2017
Chilling hours (CH) for floral emergence (cv Jintao)	$\text{CH} < 1013$			$\text{CH} \geq 1013$	274-46	Zhao et al., 2017
Chilling hours (CH) requirement (cv Hongyang)	$\text{CH} < 600$		$600 \leq \text{CH} < 700$	$\text{CH} \geq 700$	274-46	Wang et al., 2017
Chilling hours (CH) requirement (cv Hayward)	$\text{CH} < 768$			$\text{CH} \geq 768$	274-46	Wang et al., 2017
Chilling hours (CH) requirement (cv Jinyan)	$\text{CH} < 720$			$\text{CH} \geq 720$	274-46	Wang et al., 2017
Chilling hours (CH) requirement (cv Hort 16A)	$\text{CH} < 528$			$\text{CH} \geq 528$	274-46	Wang et al., 2017
Chilling hours (CH) for vegetative budbreak (cv Golden Sunshine)	$\text{CH} < 500$	$500 \leq \text{CH} < 600$	$600 \leq \text{CH} < 700$	$\text{CH} \geq 700$	274-46	Wall et al., 2008
Chilling hours (CH) for floral emergence (cv Golden Sunshine)	$\text{CH} < 700$	$700 \leq \text{CH} < 800$	$800 \leq \text{CH} < 900$	$\text{CH} \geq 900$	274-46	Wall et al., 2008
Chilling hours (CH) requirement (cv Golden Dragon)	$\text{CH} < 600$	$600 \leq \text{CH} < 700$	$700 \leq \text{CH} < 800$	$\text{CH} \geq 800$	274-46	Wall et al., 2008

Table S3. Crop's requirement table used for walnut (*Juglans regia* L.)

Parameter	Unsuitable	Marginally suitable	Suitable	Highly suitable	DoY range	Literature reference
Average temperature during the growing season	$t \leq 15\text{ }^{\circ}\text{C}$	$15 \leq t \leq 18\text{ }^{\circ}\text{C}$	$18 \leq t < 20\text{ }^{\circ}\text{C}$	$20 \leq t \leq 28\text{ }^{\circ}\text{C}$	91-305	Vahdati et al., 2019
Winter minimum temperature	$t < -20\text{ }^{\circ}\text{C}$	$-20 < t < -15\text{ }^{\circ}\text{C}$	$-15 < t < -5\text{ }^{\circ}\text{C}$	$t > -5\text{ }^{\circ}\text{C}$	335-60	Vahdati et al., 2019
Maximum temperature	$t > 38\text{ }^{\circ}\text{C}$	$35 < t \leq 38\text{ }^{\circ}\text{C}$	$30 \leq t \leq 35\text{ }^{\circ}\text{C}$	$t < 30\text{ }^{\circ}\text{C}$	1-365	Vahdati et al., 2019
Chilling hours (CH) requirement (cv Chandler)	$\text{CH} < 1015$			$\text{CH} > 1015$	274-46	McGranahan et al., 2006
Chilling hours (CH) for vegetative budbreak (cv Serr)	$\text{CH} < 650$		$650 \leq \text{CH} < 1000$	$\text{CH} \geq 1000$	274-46	Aslamarz et al., 2009
Chilling hours (CH) for floral emergence (cv Serr)	$\text{CH} < 450$		$450 \leq \text{CH} < 1000$	$\text{CH} \geq 1000$	274-46	Aslamarz et al., 2009
Chilling hours (CH) for vegetative budbreak (cv Lara)	$\text{CH} < 900$		$900 \leq \text{CH} < 1100$	$\text{CH} \geq 1100$	274-46	Aslamarz et al., 2009

Chilling hours (CH) for floral emergence (cv Lara)	CH < 750	750 ≤ CH < 1100	CH ≥ 1100	274-46	Aslamarz et al., 2009
Chilling hours (CH) for lateral vegetative budbreak (cv Pedro)	CH < 750	750 ≤ CH < 1300	CH ≥ 1300	274-46	Aslamarz et al., 2009
Chilling hours (CH) for terminal vegetative budbreak (cv Pedro)	CH < 600	600 ≤ CH < 1300	CH ≥ 1300	274-46	Aslamarz et al., 2009
Chilling hours (CH) for floral emergence (cv Pedro)	CH < 500	500 ≤ CH < 1300	CH ≥ 1300	274-46	Aslamarz et al., 2009
Chilling hours (CH) for lateral vegetative budbreak (cv Hartley)	CH < 1000	1000 ≤ CH < 1400	CH ≥ 1400	274-46	Aslamarz et al., 2009
Chilling hours (CH) for terminal vegetative budbreak (cv Hartley)	CH < 950	950 ≤ CH < 1400	CH ≥ 1400	274-46	Aslamarz et al., 2009
Chilling hours (CH) for floral emergence (cv Hartley)	CH < 750	750 ≤ CH < 1400	CH ≥ 1400	274-46	Aslamarz et al., 2009

Table S4. Crop's requirement table used for hazelnut (*Corylus avellana* L.)

Parameter	Unsuitable	Marginally suitable	Suitable	Highly suitable	DoY range	Literature reference
Average summer maximum temperature	t > 35 °C	35 ≤ t < 33 °C	33 ≤ t < 39 °C	30 ≤ t ≤ 20 °C	152-244	Malone et al., 2015
Late frost (minimum temperature)	t < -3 °C			t > -3 °C	60-121	Jha et al., 2020
Average annual temperature	t > 16 °C or t < 12 °C		12 ≤ t ≤ 13.5 °C or 14.5 ≤ t ≤ 16 °C	t < 30 °C	1-365	Ruiz-Corral et al., 2020
Maximum tolerated temperature	t > 36 °C	35 ≤ t ≤ 36		t < 35 °C	1-365	Ruiz-Corral et al., 2020
Chilling hours (CH) requirement for catkins (cv Tonda di Giffoni)	CH < 170	170 ≤ CH ≤ 200	200 ≤ CH ≤ 240	CH > 240	274-46	Mehlenbacher, 1991
Chilling hours (CH) requirement for female flowers (cv Tonda di Giffoni)	CH < 600	600 ≤ CH ≤ 640	640 ≤ CH ≤ 680	CH > 680	274-46	Mehlenbacher, 1991
Chilling hours (CH) requirement for leaf buds (cv Tonda di Giffoni)	CH < 600	600 ≤ CH ≤ 640	640 ≤ CH ≤ 680	CH > 680	274-46	Mehlenbacher, 1991
Chilling hours (CH) requirement for catkins (cv Camponica)	CH < 170	170 ≤ CH ≤ 200	200 ≤ CH ≤ 240	CH > 240	274-46	Mehlenbacher, 1991
Chilling hours (CH) requirement for female flowers (cv Camponica)	CH < 290	290 ≤ CH ≤ 327	327 ≤ CH ≤ 365	CH > 365	274-46	Mehlenbacher, 1991
Chilling hours (CH) requirement for leaf buds (cv Camponica)	CH < 680	680 ≤ CH ≤ 720	720 ≤ CH ≤ 760	CH > 760	274-46	Mehlenbacher, 1991
Chilling hours (CH) requirement for catkins (cv Negret)	CH < 240	240 ≤ CH ≤ 265	265 ≤ CH ≤ 290	CH > 290	274-46	Mehlenbacher, 1991
Chilling hours (CH) requirement for female flowers (cv Negret)	CH < 480	480 ≤ CH ≤ 540	540 ≤ CH ≤ 600	CH > 600	274-46	Mehlenbacher, 1991
Chilling hours (CH) requirement for leaf buds (cv Negret)	CH < 760	760 ≤ CH ≤ 810	810 ≤ CH ≤ 860	CH > 860	274-46	Mehlenbacher, 1991
Chilling hours (CH) requirement for catkins (cv Barcelona)	CH < 240	240 ≤ CH ≤ 265	265 ≤ CH ≤ 290	CH > 290	274-46	Mehlenbacher, 1991

<b>Chilling hours (CH) requirement for female flowers (cv Barcelona)</b>	CH < 600	$600 \leq \text{CH} \leq 640$	$640 \leq \text{CH} \leq 680$	CH > 680	274-46	Mehlenbacher, 1991
<b>Chilling hours (CH) requirement for leaf buds (cv Barcelona)</b>	CH < 990	$990 \leq \text{CH} \leq 1015$	$1015 \leq \text{CH} \leq 1040$	CH > 1040	274-46	Mehlenbacher, 1991
<b>Chilling hours (CH) requirement for catkins (cv Tonda Romana)</b>	CH < 100	$100 \leq \text{CH} \leq 135$	$135 \leq \text{CH} \leq 170$	CH > 170	274-46	Mehlenbacher, 1991
<b>Chilling hours (CH) requirement for female flowers (cv Tonda Romana)</b>	CH < 760	$760 \leq \text{CH} \leq 810$	$810 \leq \text{CH} \leq 860$	CH > 860	274-46	Mehlenbacher, 1991
<b>Chilling hours (CH) requirement for leaf buds (cv Tonda Romana)</b>	CH < 1040	$1040 \leq \text{CH} \leq 1105$	$1105 \leq \text{CH} \leq 1170$	CH > 1170	274-46	Mehlenbacher, 1991